HISTORICAL EVOLUTION OF THE COLUMBIA RIVER LITTORAL CELL

George M. Kaminsky[1*], Peter Ruggiero[2], Maarten Buijsman[3], Diana McCandless[1], and Guy Gelfenbaum[4]

To be submitted to: *Marine Geology* as part of the Special Issue on the Southwest Washington Coastal Erosion Study

[1]Washington State Department of Ecology, Olympia,WA, USA; gkam461@ecy.wa.gov
[2]Oregon State University, Corvallis, OR, USA; ruggierp@geo.oregonstate.edu
[3] University of California Los Angeles, Los Angeles, CA, USA; mbui@atmos.ucla.edu
[4]U.S. Geological Survey, Menlo Park, CA, USA; ggelfenbaum@usgs.gov

[*]Corresponding Author

Abstract
This paper details the historical coastal evolution of the Columbia River littoral cell in the Pacific Northwest of the United States. Geological data from A.D. 1700 and records leading up to the late 1800s provide insights to the natural system dynamics prior to significant human intervention, most notably jetty construction between 1885 and 1917. All reliable surveys, charts, and aerial photos are used to quantify decadal-scale changes at the three estuary entrances and four sub-cells of the littoral cell. Shoreline, bathymetric, and topographic change over three historical intervals—1870s–1920s, 1920s–1950s, and 1950s–1990s—are integrated to provide an understanding of sediment-sharing relationships among the littoral cell components. Regional morphological change data are developed for alongshore segments of approximately 5 km, enabling comparisons of shoreline change to upper-shoreface and barrier volume change within common compartments. The construction of entrance jetties at the Columbia River (1885–1917) and Grays Harbor (1898–1916) has profoundly affected the evolution of the littoral cell, and has accentuated the morphological coupling between the inlets, ebb-tidal deltas, shorefaces, and barriers. The jetties induced erosion of the inlets and offshore migration of ebb-tidal deltas. The change in boundary conditions at the entrances enabled waves to rework the flanks of ebb-tidal deltas and supply enormous quantities of sand to the adjacent coasts. Over several decades the initial sand pulses have been dispersed alongshore up to tens of kilometers from the estuary entrances. Winter waves and coastal currents produce net northward sediment transport across the shoreface while summer conditions tend to induce onshore sediment transport and accumulation of the upper shoreface and barriers at relatively high rates. Historical shoreline progradation rates since jetty construction are approximately double the late prehistoric rates between

1700 and the 1870s. Erosion rates of the mid- to lower shoreface to the south of the jettied estuary entrances have typically been greater than the accumulation rates of the upper shoreface and barrier, suggesting that the lower shoreface has been an important source of littoral sediments over decadal and longer time scales. Until recent decades, sediment supply from the ebb-tidal delta flanks and lower shoreface has largely masked the decline in Columbia River sediment supply due to flow regulation and dredging disposal practices. With the contemporary onset and expansion of coastal erosion adjacent to the jettied estuary entrances, proper management of dredged sediment is imperative to mitigate the effects of a declining sediment budget.

Keywords
shoreline change, sediment budget, coastal evolution, large-scale coastal behaviour, Columbia River littoral cell, Washington State, Oregon State

1.0 INTRODUCTION

1.1. Study Motivation

Shoreline mapping is a basic societal need because it supports many functions including legal boundaries, land-use planning and regulation, property insurance, navigational charts, and vulnerability assessments. As essential as the shoreline is to a well-functioning society, shoreline delineation and change analysis can be relatively complex endeavors. Even when a precise definition of 'shoreline' is used, it is nevertheless a sometimes amorphous feature that can make interpretation difficult. It fluctuates over all time scales in response to changes in: relative sea level; littoral sediment transport gradients; cross-shore gradients over the shoreface; and the balance of the sediment budget from sources (e.g., fluvial, estuarine, marine) and sinks (e.g., backbarrier, submarine canyons). This natural variability, when combined with mapping error and inconsistent interpretations, present many challenges in accurately assessing coastal change (Crowell et al., 1991; Moore, 2000; Ruggiero et al., 2003a).

Despite the importance of shoreline delineation, the shoreline is often an inadequate representation of the coast, which has three-dimensional sub-aerial and sub-aqueous morphology of varying composition. In general, the time scale of morphological change increases with distance offshore from the shoreline (Niedoroda and Swift, 1991; Stive and de Vriend, 1995; Nicholls et al., 1998; Cowell et al., 1999). However, changes in the offshore portion of the planform (i.e., the lower shoreface and continental shelf) have a disproportionately large influence on the upper shoreface, due to cross-shore length scales and mass continuity for sediment exchanges between the two zones (Roy et al.,

1994; Cowell et al., 1999). The morphological coupling of the offshore and nearshore zones implies the need for a systems framework which integrates this interaction in order to predict large-scale coastal behaviour (decades or longer).

Cowell et al. (2003a) propose using a composite morphology within a systems framework, collectively referred to as the 'coastal tract,' as a way of assimilating the hierarchical nature of coastal systems. The coastal tract is the first-order system (i.e., system of interest) that accounts for morphological coupling and internal dynamics that extend from the lower shoreface across the upper shoreface and barrier to the backbarrier. The lower-order system (i.e., the larger environment) sets boundary conditions for the first-order system, while higher-order components transfer residual effects to the first-order system. In practical terms, the coastal tract specifies coherent morphodynamic systems and provides a way to integrate coastal-change models across multiple temporal and spatial scales.

Using this coastal tract framework, this study focuses on the Columbia River littoral cell (CRLC; Fig. 1) as the sediment-sharing system of interest. The study examines historical evolution spanning decades to centuries and an active zone of morphologic change that extends landward from approximately 40 m water depth across the lower shoreface and barrier to the estuary. This zone encompasses the morphological system composed of Columbia River sand (less than 10 percent silt); seaward of this zone mud deposits tend to increase significantly (Nittrouer and Sternberg, 1981; Twichell et al., this issue). Gross et al. (1969) infer a predominant onshore component of sand transport in less than

40 m water depth along southwest Washington. Smith and Hopkins (1972) and Harlett and Kulm (1973) hypothesize that coarse sediments are essentially trapped in the nearshore as a result of strong wave-dominated onshore transport along the bottom, while fine sediments are winnowed and transported offshore as suspended load toward the mid-shelf. This hypothesis is consistent with observations and modeling of the northern California continental shelf, which suggest that cross-shore gradation in sediment size may result from net erosion and offshore transport of coarse silt and fine sand in water depths shallower than 50 m (Harris and Wiberg, 2002).

This study combines historical shoreline change analysis with a sediment-budget approach to quantify the historical evolution of the CRLC over three intervals (1870s–1920s, 1920s–1950s, and 1950s–1999). In addition, shoreline changes prior to significant human influence (1700–1870s) are also calculated. Data from these intervals are supplemented with additional shoreline data at sub-decadal scale, where needed and available. The additional shoreline data allow for a higher-resolution assessment of sub-interval changes and help to distinguish fluctuations from mean trends. The trends and patterns of change evidenced in historical shoreline and bathymetric data are used to infer net sediment sources, sinks, and transport pathways.

The overarching goal of the study is to develop a better understanding of, and an ability to predict, large-scale coastal behaviour to more effectively and sustainably manage the coast. The CRLC offers a superb natural laboratory for this study owing to its sedimentary system of prograded barriers, depositional estuaries, abundant sediment

supply, high energy regime, and large morphological changes as a result of high sediment transport rates, active-margin dynamics, and human interventions. The primary objective is to derive reliable change rates from morphological compartments within the first-order sediment-sharing system (i.e., the CRLC) to better understand the interactions among the estuary, inlet, ebb-tidal delta, barrier, upper shoreface, and lower shoreface. A secondary objective is to compare changes over the period prior to significant human influence (1700–1870s) with those of the modern era when human interventions began to alter natural processes. This study addresses several key questions:

- How has the littoral cell evolved over space and time?
- What relationships among the estuaries, inlets, ebb-tidal deltas, shoreface, and shoreline can be inferred from morphology change patterns?
- What sediment sources and pathways may explain historical shoreline progradation?
- What processes may explain the onset of an erosion trend along shorelines that historically prograded?
- What are the spatial and temporal effects of jetty construction at two inlets?
- How important is management of dredged material to coastal evolution?

1.2 Regional Setting

Stretching between Tillamook Head, Oregon and Point Grenville, Washington in the Pacific Northwest of the United States, the CRLC comprises the geographic extent in which modern Columbia River sediment is deposited on the beaches; the beaches to the south and north receive insignificant quantities of modern Columbia River sediment

(Clemens and Komar, 1988; Venkatarathnam and McManus, 1973). The 165-km littoral cell comprises four barrier sub-cells separated by the Columbia River and two large estuaries to the north: Willapa Bay and Grays Harbor (Fig. 1). The modern barriers and strand plains of the CRLC built up sequentially following the filling of shelf and estuary accommodation space and the onset of a relatively slow rate of eustatic sea-level rise approximately 6000 years ago (Peterson et al., this issue (a)). Approximately 4500 years ago, Long Beach and Clatsop Plains began to prograde, whereas Grayland Plains began to prograde about 2800 years ago, while the oldest portions of North Beach have sustained net progradation only for the last 2500 years (Peterson et al., this issue (b)).

The CRLC is situated along an active tectonic margin of the Cascadia subduction zone that produces large earthquakes (magnitude $\geq$ 8) at approximately 500-yr recurrence intervals (Atwater and Hemphill-Haley, 1997). These episodic events cause coseismic coastal subsidence of 0.5 to 2.5 m (Atwater, 1996) and shoreline retreat on the order of a few hundred meters (Doyle, 1996; Peterson et al., 2000). Scarp formations in the subsurface of the CRLC barriers and strand plains (detected with Ground Penetrating Radar) provide evidence of this coastal subsidence (Meyers et al., 1996; Jol et al., 1996; Peterson et al., this issue (b)). Meyers et al. (1996) and Woxell (1998) correlate the most seaward and recent paleoscarp to the A.D. 1700 Cascadia earthquake subsidence event on January 26, 1700 (Satake et al., 1996; Atwater et al., 2005).

Despite these multicentury-scale coseismic subsidence events, the CRLC barriers and strand plains have experienced net progradation (~0.5 m/yr) over the past few thousand

years partly due to interseismic rebound, a large supply of fine sand delivered by the Columbia River (Woxell, 1998; Peterson et al., 1999), and a relatively intense wave climate capable of transporting the available sediment (Tillotsen and Komar, 1997; Allan and Komar, 2000, 2006).

The wave climate along the U.S. Pacific Northwest coast is known for its severity (Tillotson and Komar, 1997), with winter storms commonly generating deep-water significant wave heights greater than 10 m (approximately one event of this magnitude per year). The largest storms in the region have produced significant wave heights in the range of 14 to 15 m (Allan and Komar, 2002). High and long-period waves (averaging approximately 3 m in height and 12–13 s in period), high mean-water levels, and a west-southwest direction of wave approach characterize the winter months (November through February), while smaller waves (1.2 m and 8 s), lower mean-water levels (approximately 30 cm lower than during winter), and wind and waves from the west-northwest characterize the summer months (May through August) (Ruggiero et al., 2005). The combination of large waves and fine sand give the CRLC its morphodynamic classification of 'modally dissipative' (Wright and Short, 1983; Ruggiero et al., 2005) in which low-frequency infragravity energy dominates the inner surf and swash zone (Ruggiero et al., 2004). Tides along the CRLC are mixed semi-diurnal ranging from 2–4 m (meso-tidal) with spring tides ranging up to approximately 4 m.

The major drivers of sediment transport along the CRLC include wave-induced orbital motions and longshore currents driven by local wind and waves. The largest waves and

strongest wind-driven currents tend to occur simultaneously during winter to produce net northward sediment transport across the Washington shelf (Smith and Hopkins, 1972; Sternberg and McManus, 1972; Kachel and Smith, 1986, 1989). Mean near-bottom current velocities of 30 cm/s on the lower shoreface are frequently supported by wave-driven currents (Harlett and Kulm, 1973). At 30-m water depth, the threshold of grain motion is exceeded a minimum of 48 days per year due to bottom currents and 79 days per year due only to waves (Sternberg, 1986). Across the shoreface from 10–24 m water depth, near-bottom currents of up to 80 cm/s during winter and 50 cm/s during summer are common (Sherwood et al., 2001; Osborne et al., 2002). Sand typical of the beach and upper shoreface (0.18 mm) is primarily transported as bedload by wave-driven near-bottom currents between 29 and 90 cm/s (Sternberg et al., 1979). Bedload transport of this coarser shoreface sand tends to be directed onshore due to asymmetry in wave-orbital velocities (Smith and Hopkins, 1972; Sherwood et al., 2001). In contrast, very fine sand (0.125–0.063 mm) is winnowed from the shoreface, transported northward and offshore as suspended load, and deposited across the mid- to outer shelf (Kachel and Smith, 1989). Sediment transport processes in the CRLC can also be influenced by tidal currents, density currents, continental shelf circulation, Ekman transport, coastal upwelling and downwelling circulation, river discharge, and plume dynamics (Creager and Sternberg, 1972; Hickey and Banas, 2003; Hickey et al., 2005; Sherwood et al., 2006; Styles, 2006; Spahn et al., in press).

1.3 Early Recorded History of the Columbia River Littoral Cell

The Washington and Oregon coasts have been inhabited for thousands of years, and by the time Europeans arrived in the 1770s, some 6000 people were likely living along the southern Washington coast (Boyd, 1990). In contrast, the era of recorded history of the CRLC is relatively young. Much knowledge of the region's history was lost forever as native populations died from smallpox epidemics, intermittent fevers, and diseases such as tuberculosis following European arrival. Fortunately, the mid-1800s ushered in the practice of recording native stories and traditions, and accounts of important events such as Cascadia earthquakes and tsunamis have been surprisingly well preserved (Ludwin et al., 2005).

Among the earliest recorded histories of the region is Bruno Heceta's descriptive log and charting taken on August 17, 1775, from aboard the Spanish frigate Santiago off the Columbia River, which Heceta called Assumption Bay. Later, on July 5, 1788, the British trader, John Meares entered Willapa Bay, which he named Shoalwater Bay, and on May 11, 1792, Robert Gray entered the Columbia River with his ship, Columbia Rediviva. While Gray and more than a dozen other explorers mapped and charted the Columbia River and Grays Harbor, a comprehensive set of depth soundings was not collected until Sir Edward Belcher (1839) and Lieutenant Charles Wilkes (1841) charted Columbia River entrance and lower estuary. Under the command of Lieutenant Wilkes, Midshipman Henry Eld mapped Grays Harbor in 1841. In 1852, Lieutenant Commanding James Alden with the U.S. Coast Survey performed the first reliable charting of Willapa (Shoalwater) Bay.

Regardless of these early efforts, the earliest historical topographic and bathymetric surveys that can be used for quantitative change analysis were performed by the U.S. Coast Survey beginning in the 1860s. These surveys were the first to extend beyond the estuary entrances to include much of the CRLC. At the entrances to the Columbia River and Grays Harbor, bathymetric surveys by the U.S. Army Corps of Engineers beginning in the 1870s document inter-annual changes at these entrances. These surveys reveal the direct relationship between jetty construction (1885–1917) and morphologic change across the inlets, shoals, and adjacent coasts (Hickson 1922; Hickson and Rodolf, 1951).

The next regional bathymetric and shoreline mapping was performed by the U.S. Coast and Geodetic Survey in the 1920s. These data provide a post-jetty baseline from which morphological response to jetty construction can be regionally quantified. Aerial photography of the coast began in the 1940s, and the first photo-derived shoreline of the CRLC was completed by the National Ocean Service in the 1950s. Since that era, CRLC shorelines have been mapped from aerial photos at approximately decadal scale, as presented in this paper.

1.4 Previous Studies

Coastal progradation generally is thought to result from allochthonous (e.g., terrigenous, river) or autochthonous (e.g., shoreface) sediment supply (Swift, 1976). In the CRLC, large barriers and strand plains (i.e., prograded barrier beaches) have been built from an abundant supply of sediment from the Columbia River (Phipps and Smith, 1978; Smith et al., 1999; Peterson et al., 1999; Peterson et al., this issue (a)). However, over the

historical period, dam construction and water irrigation have altered river flows, which have effectively reduced sand supply to the estuary by two thirds (Sherwood et al., 1990; Gelfenbaum et al., 1999). In addition to lower sediment input, reduction of peak flows has enhanced sediment accumulation within the estuary and reduced sediment discharge to the coast (Lockett, 1963; Sherwood et al., 1990). Conventional thought suggests that a reduction in Columbia River sediment supply would result in a decrease in shoreline progradation and the onset (and expansion) of coastal erosion in the littoral cell (e.g., Phipps, 1990; Galster, 2005). Phipps (1990) documents a reduction in shoreline progradation rates along much of the southwest Washington coast since the previous study (Phipps and Smith, 1978) and speculates that Columbia River dams reduced sediment discharge sufficiently to slow shoreline progradation rates.

While the effect of the dams on Columbia River sediment supply has been assumed to be the principal factor governing coastal change, jetty construction and dredging operations have also played a role (Hickson, 1922; Hickson and Rodolf, 1951; Lockett, 1959). Byrnes and Li (2001) find that jetty construction at the Columbia River entrance induced: offshore and northward migration of the ebb-tidal delta by about 3 km; shoreline progradation and shoreface accumulation along southern to central Long Beach; and shoreface erosion along northern Clatsop Plains. Moritz et al. (2003) find that jetty construction pushed 375–600 million cubic meters of sand out of the estuary between 1885 and 1925, throwing the littoral system into a state of long-term disequilibrium. They conclude that subsequent erosion of the inner delta and ebb-tidal shoals results from

equilibrium adjustments, progressive deepening of the navigation channel, and an increasingly energetic storm climate.

At the Grays Harbor entrance, Burch and Sherwood (1992) evaluate nearshore bathymetric changes related to jetty construction and rehabilitation and find the region had eroded by 117 Mm^3 between 1900 and 1990, more than half of which occurred between 1900 and 1928. Byrnes and Baker (2003) analyze shoreline change within approximately 4 km of the inlet from 1862 to 2002 over six time intervals defined by jetty construction, rehabilitation, and entrance channel deepening. They find that jetty construction produced the largest fluctuations—most notably, reversals in trend—from shoreline progradation to recession along northern Grayland Plains, and from shoreline recession to progradation along southern North Beach. They also analyze historical depth changes at the entrance and develop sediment budgets for the periods 1954/56 to 1987 and 1987 to 2002. They infer that the Grays Harbor South Jetty eliminated southward sediment supply from the inlet to the south, resulting in chronic erosion of the southern flank of the ebb-tidal delta, net northward sediment bypassing, and net accumulation of North Beach by onshore sediment transport from the ebb-tidal delta. They find that since about 1954, 40 percent of the 0.9 million cubic meters of sediment per year transported onshore from the ebb-tidal delta to North Beach gets transported southward around the North Jetty into the northern part of the entrance. Buijsman et al. (2003) perform a comprehensive historical analysis of shoreline change within 5 km of the Grays Harbor jetties. They find that shoreline fluctuations during the first several decades following jetty construction were closely correlated with changes in jetty

condition, whereas shoreline trends in recent decades correspond with the long-term morphological adjustment to jetty construction.

The Southwest Washington Coastal Erosion Study performed the first systematic processing and analysis of all regional historical shoreline and bathymetric survey data within the CRLC. Initial results are reported in Gelfenbaum et al. (1999), Gibbs and Gelfenbaum (1999), Kaminsky et al. (1999a,b), Gelfenbaum et al. (2001), Kaminsky et al. (2001), and Buijsman et al. (2003b).

2.0 DATA AND ACCOMPANYING METHODS OF ANALYSIS

This study examines the historical evolution of the CRLC based on changes in shoreline position, bathymetry, and topography using the methods described below.

2.1 Shoreline Data

Geological investigations have accurately mapped throughout the CRLC a well-constrained A.D. 1700 shoreline position (paleoscarp) resulting from an earthquake-induced subsidence event (Woxell, 1998; Peterson et al., 1999; Peterson et al., this issue (a)). This paleoscarp allows comparison of morphological change over the late prehistoric period, one of the few cases in which geological evidence allows for precise quantitative estimates of prehistoric shoreline change rates. The position of the scarp is taken to be the most landward and shallowest limit of the Ground Penetrating Radar (GPR) reflector and is interpreted to correspond in position to the toe of a modern dune

scarp. No horizontal adjustment is made to distinguish between the scarp position and a mean-high-water shoreline because they are assumed to be nearly co-located based on GPR reflectors that indicate a relatively steep beach profile at the time of scarp formation. The difference in shoreline proxy definition has relatively little effect on shoreline change rates derived over such long periods (> 150 years) along beaches experiencing coastal progradation.

Historical shoreline change rates along the entire CRLC are derived from NOS T-Sheets from the periods 1868–86, 1926–27, and 1950–57, and from aerial photographs at decadal to interannual intervals since the 1950s. Table 1 provides compartment-averaged shoreline dates. These shorelines are derived and processed using the methodologies described in Kaminsky et al. (1999a). Systematic procedures were applied to develop accurate shoreline data with consistent reference features among both T-sheets and aerial photography. Historical shoreline position error varies based on T-sheet and aerial photo mapping techniques, which include source error (±4 to ±20 m) and interpretation uncertainty (±8 to ±11 m) (Ruggiero et al., 2003a). In addition, the shoreline position uncertainty due to water level variability in the CRLC is estimated to be ±20 m (Ruggiero and List, in press). Total uncertainty in shoreline position is calculated as the square root of the sum of the squares of these errors and uncertainties, which results in a range between ±22.4 and ±29.4 m. This paper uses alongshore-averaged shoreline position data, which reduces the random source errors, so this range of total uncertainty is conservative.

Historical shoreline change is assessed using a methodology that aims to balance local-scale variability with regional-scale aggregated trends. Each sub-cell within the CRLC is divided into compartments with an average alongshore length of 5 km, varying between 1.0 and 6.3 km (Fig. 2). The compartments are categorized by sub-cell ('CP' for Clatsop Plains, 'LB' for Long Beach, 'GL' for Grayland Plains, and 'NB' for North Beach) and are arranged consecutively (c1, c2, c3,…), as in 'CPc1', 'CPc2', and 'CPc3' from south to north. Compartments immediately adjacent to estuary entrances are indicated by 'dn' for delta north (as in 'CPdn' and 'GLdn') or 'ds' for delta south (as in 'LBds' and 'NBds'). The exact boundaries and alongshore lengths of each compartment are given in Buijsman et al. (2003b). The compartment lengths are kept similar for all time intervals, except for GLc3, where a change in alongshore compartment length with each historical interval is required due to the severe erosion of Cape Shoalwater at the entrance to Willapa Bay.

Each compartment is further divided into groups representing approximately 1-km alongshore sections of shoreline. In order to compare shoreline changes over time for common shoreline reaches, the group boundaries of the 1999 shoreline are projected onto the historical shorelines to designate common shoreline reaches over time. Each group contains approximately 10 cross-shore transects at which the shoreline changes are calculated. The transects intersect each pair of sequential shorelines at approximately shore-normal orientation. All shoreline change rates presented in this paper represent averages derived from ~10 transects within the ~1 km-long groups or ~50 transects within the ~5 km-long compartments.

The regional-scale shorelines that make up the three historical intervals are complemented by additional shorelines, where needed and available, to help elucidate changes more directly associated with jetty construction. However, this study is not intended to address the local-scale responses to the jetties, which are more thoroughly addressed in the reports cited in Section 1.4.

2.2 Bathymetric Data

Bathymetric data come from the U.S. Coast and Geodetic Survey (USC&GS), National Ocean Service (NOS), the U.S. Army Corps of Engineers (USACE), the U.S. Geological Survey (USGS), and the Washington State Department of Ecology (WDOE). Data from common eras are merged to form regional bathymetric surfaces as described in Buijsman et al. (2003b). Some eras of regional-scale bathymetric data are composed of sub-regional individual surveys from different years. Because it is not practical to use multiple dates (from individual surveys) in a composite surface, a representative date for the merged bathymetry data was selected (Table 1). These dates are used for the calculation of volume change. Offsets in overlapping surveys within the same era were minimized, as were the bathymetric changes over time in deep water. Unfortunately, sparse depth soundings in some regional surveys result in irregular bathymetric surfaces that are not reliable for use in change analyses. In these cases, volume-change analysis is limited to surface areas judged to be reasonably accurate.

Bathymetric-change surfaces are derived by subtracting the bathymetric surfaces of one era from another. Bathymetric-change polygons are defined by areas with a common signal of change (erosion or accumulation) as well as the alongshore boundaries that form the compartments used in the shoreline change analysis. Bathymetric change analysis is limited to common surface areas. Furthermore, the spatial extents of the bathymetric surfaces are sometimes insufficient to capture the entire signal of first-order change. In areas where significant volume changes are clearly truncated due to limited data coverage, estimates are derived by extrapolation, proportional relations, or assumption of closure depths for upper-shoreface profile change based on bathymetric surfaces from different eras. These estimates are documented in Buijsman et al. (2003b).

2.3 Topographic Data

Topographic-change calculations for these time intervals are based on a digital elevation model (DEM) and historical shoreline positions (Buijsman et al., 2003b). Comparison of the lidar-derived DEM to ground-based field surveys indicates that the DEM underestimates actual ground elevation across the barriers and strand plains by approximately 1 m, likely due to overcompensation for vegetation heights. The topographic volume calculations presented in this paper are therefore presumed to underestimate the actual volumes contained in the barriers and strand plains, but the relative volume-changes among the compartments are not affected.

Topographic volumes are calculated above the Average High Water (AHW) shoreline (Kaminsky et al., 1999a), which is approximated by the +3.0 m NAVD 88[1] elevation contour (Ruggiero et al., 2003a). Volume changes of the prograded barrier or strand plain are calculated between historical shoreline positions using the same compartments described above for the shoreline change data. Using the same DEM for all historical intervals assumes negligible vertical change in barrier elevation over time. In the case of shoreline recession, topographic change is calculated by multiplying the eroded area by the average elevation landward of the foredune crest, assuming a beach profile of constant shape.

3.0 RESULTS OF DATA ANALYSES

This section describes in detail the results of shoreline, bathymetric, and topographic change analyses, and presents the historical evolution of the CRLC by sub-region: the mouth of the Columbia River (MCR) and adjacent coasts; the mouth of Willapa Bay (MWB); and the mouth of Grays Harbor (MGH) and adjacent coasts. Sub-regional results appear chronologically over four intervals: 1700–1870s; 1870s–1920s; 1920s–1950s; 1950s–2000. When significant gradients in shoreline change rates exist within an individual compartment, then sub-compartment (i.e., group) rates are noted in the text. Sub-interval shoreline change data are presented in figures, and only described in text as needed to clarify interval-averaged trends. Readers not interested in quantitative details

[1]NAVD 88 = North American Vertical Datum of 1988. 0.0 m NAVD 88 ranges from approximately -0.54 to -0.05 m Mean Lower Low Water (MLLW) and 2.17 to 2.51 m Mean Higher High Water (MHHW) throughout the CRLC.

of sub-regional historical evolution of the CRLC may wish to bypass this section for the summary in Section 4.0.

3.1 Historical Evolution of the Mouth of the Columbia River and Adjacent Coasts

3.1.1 MCR Morphology Change

Comparison of early historical charts (1792, 1831, 1839, 1841, and 1851) reveals insights into the morphological state of the MCR prior to significant human influence. These charts suggest a highly dynamic zone of migrating entrance channels and extensive shallow shoals. Regardless of channel position, massive shallow shoals (< 7.5 m) extended from each shore across the outer river mouth, and a large middle sand-bank typically filled much of the center of the entrance and lower estuary (Fig. 3).

The early charts show a dynamic entrance with broad, shallow shoals and two competing channels, but jetty construction between 1885 and 1917 constrained the inlet dynamics, triggering a long-term morphological response. The Columbia River South Jetty was built between 1885 and 1895 to a length of 6.8 km across the submerged Clatsop Spit (Table 2). The jetty provided limited improvement for navigation through the MCR, and it was extended seaward by an additional 4 km between 1903 and 1913. Between 1913 and 1917, the North Jetty was built to a length of 3.8 km across the large submerged Peacock Spit, reducing the width of the MCR from approximately 9.6 to 3.2 km to confine the tidal currents and deepen the entrance channel.

Between 1868 and 1926, the inlet (Compartment 6) eroded by 116.4 million cubic meters (Mm^3) (2.0 Mm^3/yr) and the inner delta (Compartment 5) eroded by 47.5 Mm^3 (0.8 Mm^3/yr) (Fig. 4a). The total volume eroded (163.9 Mm^3) is essentially identical to the volume of sand that accumulated in the estuary during the same period—164.0 Mm^3, of which 91.7 Mm^3 was in the flood-tidal shoals (Sherwood et al., 1990). The outer delta (Compartment 4) accumulated 171.5 Mm^3 (3.0 Mm^3/yr). The southern flank (Compartment 3) of the shallow ebb-tidal delta, which was cut off from the ebb-jet following construction of the South Jetty, eroded 217.5 Mm^3 (3.8 Mm^3/yr). Directly onshore, Clatsop Spit (Compartment CPdn) gained over 7 km^2 of land, accumulating 26.0 Mm^3 (0.5 Mm^3/yr). Just to the south of this area, the Clatsop Plains mid- to lower shoreface (Compartments 8 and 9) between –10 and –25 m NAVD 88 eroded by a total of 29.7 Mm^3 (0.5 Mm^3/yr), nearly balancing the accumulation of the Clatsop Plains upper shoreface (Compartments 10 and 11) of 29.2 Mm^3 (0.5 Mm^3/yr). Including this upper shoreface accumulation, Clatsop Plains south of Clatsop Spit accumulated 48 Mm^3 (0.8 Mm^3/yr). Thus, the net change south of the inlet is erosion of 173.2 Mm^3 (3.0 Mm^3/yr), which may account for the accumulation of the outer delta (Compartment 4). On the north side of the MCR, Benson Beach (Compartment LBds), a pocket beach between the MCR North Jetty and North Head, gained nearly 4 km^2 of land, accumulating 21.7 Mm^3 (0.4 Mm^3/yr). North of North Head, the Long Beach Peninsula accumulated 26.6 Mm^3 (0.5 Mm^3/yr) of sand. Due to large irregularities in the 1926 bathymetric data, nearshore bathymetric volume change along Long Beach cannot be directly calculated for this period; an invariant upper-shoreface profile to –12.2 m Mean High Water (MHW) is assumed to translate horizontally with the change in shoreline position.

Between 1926 and 1958, the inlet (Compartment 4) eroded 53.8 Mm^3 (1.7 Mm^3/yr) and the inner delta (Compartment 6) eroded 54.2 Mm^3 (1.7 Mm^3/yr) (Fig. 4b). Sherwood et al. (1990) report sand accumulation in the estuary (77.9 Mm^3; 2.4 Mm^3/yr) and flood-tidal shoals (33.5 Mm^3; 1.1 Mm^3/yr) during this time, totaling 111.4 Mm^3 (3.5 Mm^3/yr). Including the accumulation of 3.7 Mm^3 (0.1 Mm^3/yr) along Clatsop Spit within the inlet (Compartment 5), erosion of the inlet and inner delta aggregates to 104.2 Mm^3 (3.3 Mm^3/yr). Nearly all of this erosion can be accounted for in the outer delta (Compartment 7), which accumulated 101.3 Mm^3 (3.2 Mm^3/yr). However, an accumulation zone (Compartment 23) of 113.5 Mm^3 (3.6 Mm^3/yr) fans out to the northwest from the outer delta toward the mid-shelf silt deposit (Nittrouer and Sternberg, 1981). The source of this accumulation can only partially be accounted for by the net erosion of 25.1 Mm^3 (0.8 Mm^3/yr) from south of the inlet. Buijsman et al. (2003b) hypothesize that this accumulation may be composed of fine sediment released from the Columbia River during a large flood in 1948.

South of the MCR, an offshore zone (Compartment 22) from approximately –55 m to –23 m NAVD 88 displays localized fluctuations of up to a few meters of erosion and accumulation, with net volume gain of 32.0 Mm^3 (1.0 Mm^3/yr). A mid- to lower shoreface zone (Compartments 11, 12, 13, and 14) between approximately –23 and –10 m NAVD 88 reveals significant erosion of 72.3 Mm^3 (2.3 Mm^3/yr). Nearly 60 percent of this erosion occurred across the southern flank (Compartment 11) of the ebb shoal separated from the inlet by the Columbia River South Jetty. Onshore of the ebb-shoal

erosion, the upper shoreface (Compartments 9 and 10) and Clatsop Spit (Compartment 8) also eroded by a total of 14.0 Mm^3 (0.4 Mm^3/yr). To the south, the upper shoreface (Compartments 19, 20, and 21) accreted 14.9 Mm^3 (0.5 Mm^3/yr), accounting for half of the erosion that occurred directly offshore on the mid- to lower shoreface. Clatsop Plains experienced net accumulation with increasing rates toward the center at Compartment CPc3. Excluding erosion of Clatsop Spit (Compartment 8) by 4.6 Mm^3 (0.2 Mm^3/yr), Clatsop Plains accumulated 61.2 Mm^3 (1.9 Mm^3/yr).

Nearly all bathymetric areas north of the MCR experienced net accumulation. The one exception was an area of minimal change (Compartment 15), in which there was 5.4 Mm^3 (0.2 Mm^3/yr) net erosion. From approximately –23 to –10 m NAVD 88 depth is a moderate accretion band (Compartment 16) that accumulated 12.8 Mm^3 (0.4 Mm^3/yr). Extending northward and onshore from the outer delta is a nearshore corridor (Compartment 3) of moderate accumulation (8.3 Mm^3; 0.3 Mm^3/yr) that connects to the upper shoreface. From the North Jetty to 14.7 km northward, the upper shoreface (Compartments 2, 17, and 18) accumulated 49.5 Mm^3 (1.6 Mm^3/yr).

As with the previous two time intervals, the inlet and inner delta (Compartment 2) continued to erode between 1958 and 1999, but complete bathymetric coverage of the inlet was lacking in 1999 (Fig. 4c). The inner-delta erosion expanded westward and northward during this period to include Peacock Spit (Compartment 1), with a combined loss of 54.6 Mm^3 (1.3 Mm^3/yr), despite the placement of 40.7 Mm^3 of dredged material in Disposal Site E during this interval (USACE, 1999). The outer delta (Compartment 3)

continued to migrate to the northwest, accumulating 45.1 Mm^3 (1.1 Mm^3/yr), not including the southern lobe (Compartment 6), which includes dredged material Disposal Site B. During this interval, 52.1 Mm^3 of dredged material was placed at Disposal Site B (USACE, 1999) while the bathymetric change shows accumulation of 45.8 Mm^3, about 90 percent of the total disposed. Two other disposal sites (F and A) to the southeast of Site B appear as islands of accumulation surrounded by zones of erosion. The deeper of the two, Site F (Compartment 7), received 7.5 Mm^3 of dredged material and retained about one-half that amount. In shallower water, Site A (Compartment 5) received 28.8 Mm^3 and retained just under one-quarter of that amount. Most of the disposed material came from the entrance channel within the inlet. The southern flank (Compartment 13) of the ebb-tidal delta eroded 30.3 Mm^3 (0.7 Mm^3/yr), and the Clatsop Plains mid- to lower shoreface (Compartment 14) eroded 25.8 Mm^3 (0.6 Mm^3/yr). Clatsop Plains accumulated 50.9 Mm^3 (1.2 Mm^3/yr), including 21.3 Mm^3 (0.5 Mm^3/yr) on the upper shoreface (Compartments 12, 17, 18, and 19). The southern Long Beach shoreface (Compartments 8, 9, 15, and 16) shallower than –23 m NAVD 88 accumulated 67.8 Mm^3 (1.7 Mm^3/yr). Over the total length of Long Beach, the upper shoreface and barrier accumulated a total of 127.0 Mm^3 (3.1 Mm^3/yr).

Over the entire period from 1868 to 2000, the MCR inner delta deepened by 10.1 m. The deepening rate slowed over time from 12.0 cm/yr between 1868 and 1926, to 6.4 cm/yr between 1926 and 1958, and to 2.6 cm/yr between 1958 and 2000. Although the rate slowed, the area of inner-delta erosion expanded seaward from 6.9 km^2 to 26.5 km^2 to 43.5 km^2 over these three intervals. As the inner-delta erosion expanded over the area of

outer delta accumulation of the first interval (Compartment 4 in Fig. 4a), the outer-delta depocenter migrated 3.3 km to the west-northwest, with the outer delta accumulating more sediment than had eroded from the inner delta.

Over the entire historical period, the southern flank of the ebb-tidal delta—upon which the Columbia River South Jetty was constructed—lowered by decreasing rates over time, from 7.6 cm/yr during the first interval, to 4.5 cm/yr during second interval, and to 1.8 cm/yr during third interval. Thus, the decrease in the rate of lowering of the southern flank is similar to the slowing of the inner-delta erosion. Whereas the inner-delta erosion slowed as the outer-delta depocenter migrated offshore, along Clatsop Plains, the rate of lowering of the southern flank slowed as the barrier depocenter migrated southward (Fig. 4c).

3.1.2 Clatsop Plains Shoreline and Volume Changes

Shoreline progradation rates along Clatsop Plains vary significantly over time and space. Between the A.D. 1700 paleoscarp and the pre-jetty shorelines of 1868 to 1874 (Table 1), a moderate alongshore gradient in shoreline progradation rates range from a high of 2.2 m/yr near the MCR to a low of 0.9 m/yr in southern Clatsop Plains (Fig. 5). Between 1868 and 1926, shoreline progradation rates increase dramatically near the South Jetty at Compartment CPdn, averaging 28.9 m/yr. The jump in shoreline progradation rates is even higher based on sub-interval shoreline data (Figs. 6 and 7). Between 1868 and 1892, the shoreline at CPdn progrades only 3.3 m/yr, then increases to 46.9 m/yr between 1892 and 1926. Compared to the 1926 shoreline, the 1910 shoreline shown in the

USACE survey is approximately 500 m seaward at the jetty and 100 m seaward at the middle of CPdn (Fig. 6); thus, even higher shoreline progradation rates would be calculated near the South Jetty using shoreline data from 1892 and 1910. The shoreline changes at CPdn between 1868 and 1926 equate to 37.7 $m^3/yr\ m^{-1}$ of sediment accumulation above MHW (Table 3).

The shoreline change (and strand plain and upper shoreface accumulation) rates for 1868–1926 decrease substantially with distance from the jetty, from 8.2 m/yr (121.0 $m^3/yr\ m^{-1}$) at CPc5 to 3.3 m/yr (79.7 $m^3/yr\ m^{-1}$) at CPc4 (Fig. 5, Table 3). Group-averaged shoreline progradation rates taper to zero at the southern boundary of CPc4, and shoreline and volume changes farther south are minimal.

Regional shoreline changes along Clatsop Plains between 1926 and 1957 make a clockwise rotation around a pivot point roughly 5.1 km south of the South Jetty. The group-averaged shoreline recession rates within CPdn from north to south are 8.7, 5.3, and 1.8 m/yr; the compartment-averaged shoreline recession rate is 5.8 m/yr with the beach above MHW eroding by 17.5 $m^3/yr\ m^{-1}$. South of the pivot point, rates of shoreline progradation and strand plain accumulation increase across CPc5, CPc4, and CPc3 to a peak of 12.0 m/yr and 121.6 $m^3/yr\ m^{-1}$ at CPc3, respectively (Fig. 5, Table 3). The two compartments to the south, CPc2 and CPc1, lack shoreline data from the 1950s, but substituting 1962 data shows declining shoreline progradation rates from 6.2 to 4.2 m/yr for CPc2 and CPc1, respectively. Upper shoreface and strand plain accumulation

rates for CPc2 and CPc1 are estimated to be 107.4 and 43.7 $m^3/yr\ m^{-1}$, respectively (Buijsman et al., 2003b).

Between the 1950s[2] and 1999, the shoreline receded slightly near the Columbia River South Jetty, and prograded modestly toward central Clatsop Plains (Fig. 5). From north to south the shoreline receded 0.1 m/yr at CPdn, then prograded 0.1 m/yr at CPc5, increasing to 1.8 m/yr at CPc4. Farther south the shoreline prograded 1.6 m/yr at CPc3 and CPc2, and then slowed to 0.9 m/yr at CPc1. The upper shoreface and strand plain accumulated at increasing rates ranging from 16.4 $m^3/yr\ m^{-1}$ at CPc5 to 86.0 $m^3/yr\ m^{-1}$ at CPc3, then at decreasing rates to 30.9 $m^3/yr\ m^{-1}$ at CPc1 (Table 3).

3.1.3 Long Beach Shoreline and Volume Changes

Along the Long Beach Peninsula, shoreline change rates between 1700 and the 1870s average as low as 0.3 m/yr at the southern end and consistently increase with distance northward (Fig. 5). Spit growth occurred to the north with compartment-averaged rates of 7.1 m/yr in LBc7 to 21.3 m/yr in LBdn. Maximum shoreline progradation occurred at the northern tip with a group-averaged rate of 25.8 m/yr (i.e., 4.4 km of spit growth).

According to USACE annual surveys at the MCR, shoreline change rates along Long Beach remained steady until the North Jetty was constructed. The initial shoreline response was confined to the development of the pocket beach between the jetty and North Head (i.e., within LBds) (Fig. 6). Averaged over 1869–1926, the shoreline progradation rate for LBds is 18.4 m/yr (39.3 $m^3/yr\ m^{-1}$ above MHW), but given that the

[2] 1962 shoreline is used for CPc2 and CPc1.

shoreline at the base of this headland did not begin to prograde until after 1914, and considering that this emerged beach formed by rapid accumulation along the north-side toe of the jetty, the shoreline prograded toward the northwest by 53.9 m/yr between 1914 and 1926.

Not until after 1926 does the shoreline to the north of North Head appear to have been significantly affected by the changes at the MCR (Fig. 6). Shoreline progradation rates along southern and central Long Beach between the 1870s and 1926 are only slightly higher than the rates during the late prehistoric period from 1700 to the 1870s (Fig. 5). Similarly, the upper shoreface and barrier in the first four compartments north of North Head accumulated at relatively uniform rates on the order of 17 $m^3/yr\ m^{-1}$ between the 1870s and 1926 (Table 3). The rates of both shoreline progradation and upper shoreface and barrier accumulation are slightly higher at LBc5, then lower to the north at LBc6 and reverse to erosion at LBc7. The northern end of the spit (LBdn) grew northward, as will be presented in greater detail in Section 3.2.

Between 1926 and the 1950s, Long Beach experienced large-scale shoreline rotation, with the inflection point located approximately 25 km north of the Columbia River North Jetty (between LBc4 and LBc5) (Fig. 5, Table 3). Both shoreline and volume-change rates show similar trends, with highest rates of progradation and accumulation at the southern end (14.0 m/yr at LBds and 193.9 $m^3/yr\ m^{-1}$ at LBc1) and highest rates of erosion near the northern end (6.9 m/yr and 65.4 $m^3/yr\ m^{-1}$ at LBc7). The barrier accumulation along southern Long Beach (LBc1 to LBc4) totals 76 Mm^3 (2.4 Mm^3/yr),

and the erosion along northern Long Beach (LBc5 to LBdn) totals 24.3 Mm^3 (0.8 Mm^3/yr), resulting in net volume change of 51.7 Mm^3 (1.6 Mm^3/yr) for Long Beach—excluding LBds, which accumulated 5.6 Mm^3 (0.2 Mm^3/yr) landward of MHW.

Between the 1950s and 1999, the southernmost compartment (LBds) eroded by 8.2 m/yr (22.8 m^3/yr m^{-1} above MHW), reversing its trend from the previous interval. Along the rest of southern Long Beach (LBc1 and LBc2), rates of shoreline progradation and upper shoreface and barrier accumulation increase with distance to the north, but are lower than during the previous interval (Fig. 5, Table 3).

Over the entire historical period, sediment accumulation volumes along Long Beach increased from 48.3 Mm^3 between 1869 and 1926, to 57.3 Mm^3 between 1926 and the 1950s, and to 127.0 Mm^3 between the 1950s and 1999. As the total volume of accumulation along Long Beach increased over time, the depocenter of accumulation migrated northward. Initially the depocenter was located at LBds (based on shoreline progradation rates of 18.4 m/yr from 1869–1926 and 53.9 m/yr from 1914–1926, and rapid accumulation of the upper shoreface as part of the shore-connected ebb shoal, as shown in Fig. 4a). Between 1926 and the 1950s, the depocenter was farther north, within LBc1, where accretion rates were 13.7 m/yr and 193.9 m^3/yr m^{-1}. Between the 1950s and 1999, the depocenter was even farther north, between LBc2 and LBc3, where accretion rates were approximately 5.5 m/yr and 110.6 m^3/yr m^{-1}. All rates of shoreline progradation and upper shoreface and barrier accumulation along central to northern Long Beach (LBc3 to LBdn) between the 1950s and 1999 were higher than the earlier

historical rates since 1871. Only between 1700 and 1871 along northern Long Beach (LBc6 to LBdn) were shoreline progradation rates higher than those between the 1950s and 1999.

3.2 Historical Evolution of the Mouth of Willapa Bay

Since 1852, when the U.S. Coast Survey first mapped Willapa (Shoalwater) Bay, the shorelines, shoals, and entrance channel positions have substantially changed. Between 1852 and 1871, spits from both the north (Cape Shoalwater) and south (Leadbetter Point) grew significantly toward the center, largely emerging from shallow shoals that existed in 1852 (Fig. 8a).

The 1890 and 1891 USC&GS hydrographic surveys include a 1891 shoreline survey of Leadbetter Point and Cape Shoalwater that enables the first quantitative shoreline change analyses at the MWB. At the northernmost tip of Leadbetter Point, the group-averaged shoreline progradation rate is 15.6 m/yr between 1871 and 1891. Along Cape Shoalwater (GLc2 in Fig. 9), the compartment-averaged shoreline recession rate is 12.5 m/yr; within this compartment from east to west, the group-averaged recession rates are 23.9, 20.1, 13.5, and 6.8 m/yr. The 1890 and 1891 bathymetric surveys show an extended Long Beach shoal 3.5 km north of Leadbetter Point holding the entrance channel to within 1.3 km of Cape Shoalwater (Fig. 8a).

Between 1891 and 1911, the northern tip of the Leadbetter Point shoreline receded by 16.8 m/yr, but the shoal extending from Leadbetter Point continued its northward expansion, extending 300 to 600 m north of its 1891 position and widening toward the northeast by as much as 1.1 km (Fig. 8a). In 1911, this shoal was as close as 200 m south of the southernmost point of the 1871 Cape Shoalwater shoreline and confined the entrance channel to be as narrow as 1.5 km between the north-northeastern edge of the shoal and the Cape Shoalwater shoreline. From the southernmost point of the 1891 Cape Shoalwater shoreline to approximately 3.5 km westward, the group-averaged shoreline recession rates between 1891 and 1911 are 50.3, 41.2, and 2.5 m/yr, with the most western group split between recession to the east and progradation to the north. At the outermost point along the northern entrance to the bay, the south-southwest-facing shoreline of 1911 took an abrupt turn to face west (Fig. 8a). Northward from this point within approximately 4.5 km the shoreline prograded between 1891 and 1911 with group-averaged rates of 15.4, 12.3, and 8.5 m/yr. The Willapa Bay lighthouse, located on a sand knoll (approximately 14 m above MSL) near the terminus of a ridge extending along Grayland Plains (Cooper, 1958), remained nearly 1.2 km from the northward-receding shoreline in 1911.

Between 1911 and 1926, Cape Shoalwater shoreline receded 23.1 m/yr along the 3.8 km of south-southwest facing shoreline (GLc2 in Fig. 9); from east to west within this compartment, group-averaged shoreline recession rates are 40.0, 32.4, 39.1, and 8.3 m/yr). At Leadbetter Point, the northwestern tip did not significantly change position, while the shoreline to the west along LBdn receded by 10.2 m/yr. Averaged over 1871–

1926, the northwest tip of Leadbetter Point receded by 0.4 m/yr, while the adjacent groups prograded by 3.4 and 2.3 m/yr.

USACE surveys show that by 1928 the shoal extending north from Leadbetter Point had transgressed the 1871 shoreline at Cape Shoalwater (Fig. 8a). Additionally, the entrance channel had migrated northward, scouring a deep thalweg where the large 1891 arm of the cape had reached into the bay.

The morphological change of the MWB is well documented in nearly annual USACE bathymetric surveys from 1928 through 1978 (e.g., Hands, 2000b). These surveys show that the main entrance channel continued to migrate northward along with the northward expansion of the shoals extending from Leadbetter Point. Terich and Levenseller (1986) and Hands (2000a) describe a cyclic pattern evident in the surveys where: 1) the northern shore-connected shoal grows toward the southwest, forcing the entrance channel to bend sharply to the southwest; 2) the northern entrance channel breaches the shoal near this sharp bend; 3) the distal end of the breached shoal migrates to the southeast across the abandoned channel to merge with the entrance shoal extending from Leadbetter Point; 4) the enlarged shoal in the middle of the entrance forces the northern entrance channel to migrate northward; and 5) the northern channel erodes Cape Shoalwater, supplying sediment to the northern shore-connected entrance shoal, which re-initiates this sequence. Hands (2000a) identifies seven cycles between 1933 and 1998. The time series of USACE surveys reveal that breaching of the northern shore-connected shoal typically

begins with the development of incipient outlet over several years until a critical depth of approximately 6 m is reached.

Between 1926 and 1950, both Leadbetter Point and Cape Shoalwater shorelines receded (Fig. 8a). At Leadbetter Point, the shoreline receded 13.8 m/yr along the northernmost point, decreasing to the west from 11.9 to 4.0 m/yr. The Cape Shoalwater shoreline (GLc2 in Fig. 9) receded 34.4 m/yr; from east to west within this compartment, group-averaged shoreline recession rates are 35.6, 46.7, 49.2, and 15.5 m/yr.

The Leadbetter Point shoreline continued to recede between 1950 and 1963 by as much as 50.9 m/yr before reversing to rapid progradation between 1963 and 1974 by as much as 107.6 m/yr (Figs. 7 and 8b). The shoreline progradation rates slow over time. Averaged over 1963 to 1999, the shoreline prograded 54.1 m/yr along the most northern point, 53.0 m/yr toward the north northwest, 28.8 m/yr toward the northwest, and 10.0 m/yr toward the west-northwest.

The Cape Shoalwater shoreline within GLc2 receded by 22.9 m/yr between 1950 and 1963. Between 1963 and 1974, this shoreline receded by 37.3 m/yr, the highest compartment-averaged rate between successive historical shorelines at GLc2. Since 1974, the shoreline recession rates progressively slowed from 18.5 m/yr between 1974 and 1987 to 13.3 m/yr between 1995 and 1999 (Fig. 9). Nevertheless, along the southernmost group within GLc3, the shoreline receded by more than 30 m/yr during the 1990s as the channel breached the northern shoal. Averaged over 1950 to 1999, within

GLc2 from east to west, the group-averaged shoreline recession rates are 19.9, 25.5, and 24.3 m/yr; within the southernmost group of GLc3, the shoreline recession rate is 11.7 m/yr.

3.3 Historical Evolution of the Mouth of Grays Harbor and Adjacent Coasts

3.3.1 MGH Morphology Change

At the MGH, early historical charts (1792, 1841, and 1862) show massive shallow shoals extending from the adjacent coasts across much of the entrance, bisected only by the entrance channel. North of the entrance channel, a large recurved spit took the form of Eld Island during the mid-1800s, with a marginal tidal channel running between this island and the North Beach barrier (Fig. 10). Like the MCR surveys, the early historical MGH surveys suggest that sediment was abundant and readily shared across sub-cells and within the estuary entrance.

On the north side of the MGH, the retreat of the North Beach recurved spit, first noted between 1860 and 1886, continued up to the time of jetty construction (Fig. 11). By 1898, the USACE survey shows this spit up to 900 m closer to the southern end of the barrier than it was in 1886. Along the west-southwestern facing shoreline, the spit merged with the barrier, retreating approximately 350 m. Despite this shoreline retreat and the loss of Eld Island, the northern side of the inlet remained a shallow spit platform during the early historical period. The entrance channel ran roughly east-west between this submerged spit platform and Point Chehalis, and essentially remained stationary. In

fact, the 1898 survey shows the thalweg about 0.5 km farther south than in the 1862 survey, with the North Beach spit platform encroaching on the 1862 location of the thalweg.

On the south side of the MGH, both erosion and accretion occurred after 1886. Between 1886 and 1898, the Point Chehalis shoreline within the entrance prograded by roughly 50 m along a 1-km reach facing north-northeast, and receded by roughly 170 m along a 1-km reach facing northwest (Fig. 11). Between 1898 and 1902, the Grays Harbor South Jetty was constructed to a length of 4.2 km across the shallow shoal attached to Point Chehalis (Table 2). Between 1898 and 1909, the shoreline within the entrance prograded 9.2 m/yr, as the spit expanded both northward and westward. Between 1909 and 1926, the shoreline prograded northward 14.2 m/yr; this includes a small area of erosion that extends about 200 m alongshore immediately north of the jetty. Averaged over 1886 to 1926, Point Chehalis prograded 292 m northward at a rate of 7.3 m/yr.

On the north side of the MGH, the shoreline retreated between 1886 and 1909 by up to 49.2 m/yr within the southernmost group (Fig. 11). Between 1908 and 1916, the Grays Harbor North Jetty was built to a length of 5.2 km across the broad shoal platform attached to Point Brown, reducing the width of the entrance channel from approximately 3.7 to 2.5 km (Table 2).

Bathymetric volume-change analysis for the Grays Harbor region from the late pre-jetty to early post-jetty period was performed by merging the earliest surveys (1887 and 1900)

into a composite survey and comparing it to the 1926 survey (Fig. 12a). During this time, the inner delta (Compartment 3) eroded more than any other compartment, losing 44.7 Mm^3 (1.4 Mm^3/yr), while the inlet (Compartment 7) eroded by 39.5 Mm^3 (1.2 Mm^3/yr) (Fig. 12a). Volume changes within the estuary and flood shoals are unknown due to lack of data, but the inner harbor accreted land and became shallower as the inlet deepened. Point Chehalis (Compartment 8) accumulated 2.2 Mm^3 and Point Brown (Compartment 6) accumulated 2.5 Mm^3, a total of 4.7 Mm^3 (0.1 Mm^3/yr). The outer delta (Compartment 4) accumulated 15.0 Mm^3 (0.5 Mm^3/yr).

Annual dredging of the Grays Harbor entrance channel began in 1916, and excluding 1918 and 1919, continued through 1942. Between 1894 and 1927, approximately 5 Mm^3 (0.6 Mm^3/yr) of sediment was dredged and disposed of on the southwest flank of the ebb-tidal delta off the end of the dredged channel.

The morphological response at the MGH to jetty construction was similar to that at the MCR. Between 1893 and 1926, the southern flank (Compartment 9) of the ebb-tidal shoal at the MGH eroded by 36 Mm^3 (1.1 Mm^3/yr), and the Grayland Plains mid- to lower shoreface (Compartments 11, 12, 13, and 14) between –10 and –23 m NAVD 88 eroded by 71.9 Mm^3 (2.2 Mm^3/yr) (Fig. 12a). The upper shoreface and strand plain accreted by a total of 56.7 Mm^3 (1.7 Mm^3/yr).

Within 6 km of the North Jetty NBds, the barrier, beach, and nearshore zone all accumulated sand between 1893 and 1926, the period encompassing jetty construction.

The most inland and low-lying portion of the coast north of the North Jetty, Oyhut tidal flats (Compartment 5), accumulated 9.2 Mm^3 (0.3 Mm^3/yr) (Fig. 12a). The barrier gained approximately 8 km^2 of land, accumulating 29.8 Mm^3 (0.9 Mm^3/yr), and the upper shoreface along NBds accumulated 17 Mm^3 (0.5 Mm^3/yr). The compartments north of NBds accumulated 17.6 Mm^3 (0.9 Mm^3/yr). In total, North Beach accumulated 73.6 Mm^3 (2.2 Mm^3/yr), which can be accounted for by net erosion of the inlet (Compartment 7) and inner delta (Compartment 3), which combines to 79.5 Mm^3 (2.4 Mm^3/yr).

The MGH inlet (Compartments 6 and 7) and inner delta (Compartment 3) continued to erode between 1926 and 1954 (29.4 Mm^3; 1.1 m^3/yr), but much less than between 1893 and 1926 (Fig. 12b). Along Point Chehalis, the shoreline within the inlet receded toward the southwest by 8.6 m/yr between 1926 and 1951. This recession included the initial development after 1946 of the log-spiral embayment, Half Moon Bay (Fig. 11). Within the MGH along the North Jetty, the inner harbor spits eroded and the jetty became the boundary between land and sea.

The largest bathymetric change between 1926 and 1954 occurred in the outer delta (Compartment 4), which gained 59.7 Mm^3 (2.1 m^3/yr), about twice as much as the erosion that occurred within the entrance and inner delta combined (Fig. 12b). These changes included approximately 10 Mm^3 of sand that was dredged from the bar and entrance channels and disposed of on the southwest flank of the ebb-tidal delta between 1926 and 1942.

South of the MGH, the southern flank (Compartment 8) of the ebb-tidal delta eroded by 11.1 Mm^3 (0.4 Mm^3/yr) between 1926 and 1954, while Grayland Plains, including the upper shoreface, accumulated 11.8 Mm^3 (0.4 Mm^3/yr). The Grayland Plains mid- to lower shoreface (Compartment 11) between approximately –10 and –24 m NAVD 88 fluctuated between up to 1 m of erosion and 2 m of accumulation, with a net change of only 1.2 Mm^3.

The upper shoreface along North Beach accumulated much more than Grayland Plains during this interval. Excluding the portion interpreted to be part of the outer delta, the mid-shoreface (Compartment 12) between approximately –8 and –24 m NAVD 88 along North Beach accumulated 12.2 Mm^3 (0.4 Mm^3/yr). The upper shoreface (Compartment 2) landward of this zone accumulated 19 Mm^3 (0.7 Mm^3/yr). In total, North Beach accumulated 106.7 Mm^3 (3.8 Mm^3/yr), including the nearshore and barrier adjacent to the Grays Harbor North Jetty. These changes resulted in a significant offset in accumulation between North Beach and Grayland Plains, with North Beach accumulating roughly 8 to 10 times more sand than Grayland Plains (Fig. 11).

The MGH inlet (Compartment 10) deepened significantly between 1954 and 1999, eroding by 30.6 Mm^3 (0.7 Mm^3/yr) (Fig. 12c). The inner delta (Compartment 4) continued to expand outward from the inlet, losing 40.6 Mm^3 (0.9 Mm^3/yr), thus maintaining the same average rate as the previous interval. The outer delta (Compartment 5) accumulated 52.5 Mm^3 (1.2 Mm^3/yr), and a more diffuse zone (Compartment 6) offshore accumulated 9.9 Mm^3 (0.2 Mm^3/yr). A dredged-material

disposal site (Compartment 7) near the 40 m contour to the southwest of the entrance accumulated 1.8 Mm^3, and is adjoined by an offshore dispersion zone (Compartment 8) that accumulated 4.2 Mm^3.

Between 1943 and 1987, the Grays Harbor bar and entrance channels were not dredged. Between 1988 and 2000, 5.2 Mm^3 of sand was dredged from the bar and entrance channels, and at least 19.6 Mm^3 was dredged from the lower to mid-estuary. A total of 11.6 Mm^3 was disposed of either onshore or nearshore in the vicinity of the South Jetty. As noted above, an additional 1.8 Mm^3 was disposed of within the Southwest Ocean Disposal Site (Compartment 7) northwest of the outer bar channel.

The upper to lower shoreface (Compartments 11, 12, 14, and 15) along Grayland Plains exhibited substantial erosion totaling 53.9 Mm^3 (1.2 Mm^3/yr) between 1954 and 1999, with over half of the erosion occurring on the southern flank (Compartment 11) of the relict ebb-tidal delta (Fig. 12c). In contrast, Grayland Plains accumulated 7.3 Mm^3 (0.2 Mm^3/yr). Most of the barrier and upper-shoreface accumulation occurred along southern Grayland Plains, where the shore-connected shoal of the MWB migrated northward along with the entrance itself.

North of the MGH, the upper shoreface (Compartment 3) within 3 km of the Grays Harbor North Jetty eroded 1.6 Mm^3, while the barrier accumulated 3.1 Mm^3 between 1954 and 1999. To the north of this reach, the upper shoreface and barrier accumulated a

total of 39.2 Mm^3 (0.9 Mm^3/yr). The data reveal a regional gradient in accumulation rate that decreases from NBc1 to NBc7.

From 1900 to 1999, the average depth of the Grays Harbor inner delta increased by 6.2 m. The rate of deepening slowed slightly from 7.5 cm/yr between 1900 and 1926 to 6.9 cm/yr between 1926 and 1954. Between 1954 and 1999, the deepening rate slowed appreciably to 3.9 cm/yr as the area of erosion expanded significantly seaward.

While the inner delta eroded, the outer delta accreted and migrated offshore during each consecutive time interval. Between 1893 and 1926, the outer delta accumulated 6.0 cm/yr over an area of 7.6 km^2. Between 1926 and 1954, the rate of accumulation increased to 11.5 cm/yr, the depocenter migrated approximately 1.1 km to the northwest, and the total area increased to 18.5 km^2. Between 1954 and 1999, the outer-delta accumulation slowed to 5.1 cm/yr as the outer delta expanded to 23 km^2, not including a more diffuse zone of accumulation offshore. In total, this represents a three-fold expansion in size of the outer delta. The 1954–1999 depocenter migrated approximately 0.8 km to the west-southwest of its 1926–1954 position, and the landward edge of the outer-delta deposition band shifted to the approximate location of the seaward edge of the 1893–1926 outer-delta deposit. The resultant shift of the outer-delta depocenter from 1893–1926 to 1954–1999 was 1.6 km to the west-northwest.

Over the entire historical period from 1893 to 1999, the southern flank of the Grays Harbor ebb-tidal delta lowered by 6.8 cm/yr between 1893 and 1926, 4.1 cm/yr between

1926 and 1954, and 4.2 cm/yr between 1954 and 1999. These rates of lowering are similar to those of the southern flank of the Columbia River ebb-tidal delta during the first two intervals (7.6 and 4.5 cm/yr, respectively), but for the most recent interval (1950s–1999) the rate of lowering near Grays Harbor (4.2 cm/yr) was higher than at the southern flank of the MCR (1.8 cm/yr).

3.3.2 Grayland Plains Shoreline and Volume Changes

Between 1700 and 1886, the Grayland Plains shoreline progradation rates are highest at each end of the sub-cell (Fig. 13). At Point Chehalis, the shoreline within the entrance prograded northward 10.1 m/yr, and the westward-facing shoreline at GLdn prograded to the northwest 7.0 m/yr. While much of the shoreline progradation at Point Chehalis and GLdn occurred between 1860 and 1886, the shoreline progradation rates between 1700 and 1860 are 4.5 m/yr and 2.4 m/yr, respectively, still higher than those of central Grayland Plains between 1700 and 1886. Along southern Grayland Plains, much of the geologic record that could have given insight into the rate of spit growth during the late prehistoric period was lost with the erosion of Cape Shoalwater during the historical period. Nevertheless, between 1700 and 1880, the shoreline in southern Grayland Plains (GLc3) prograded 2.6 m/yr, compared to 1.5 m/yr averaged from central Grayland Plains (GLc4, GLc5, and GLc6).

Prior to construction of the Grays Harbor South Jetty, the 1898 shoreline position averaged 85 m landward of the 1886 shoreline at the northern end of Grayland Plains

(GLdn), representing an average recession rate of 7.1 m/yr (Fig. 9). During jetty construction between 1898 and 1902, and immediately after to 1909, the GLdn shoreline prograded an average of 633 m (57.5 m/yr). This shoreline then retreated 258 m (15.2 m/yr) by 1926. Averaged over 1886–1926, the GLdn shoreline prograded 6.4 m/yr and the upper shoreface and barrier prograded 26.4 $m^3/yr\ m^{-1}$ (Figs. 11 and 13).

In contrast to the regional shoreline change pattern between 1700 and 1886, the shoreline prograded at higher rates of up to 8.2 m/yr toward central Grayland Plains, and lower rates at each end of the sub-cell between 1886 and 1926 (Fig. 13). The upper shoreface and barrier accumulation rates increased with distance from the Grays Harbor South Jetty to a peak of 105.2 $m^3/yr\ m^{-1}$ at GLc4 (Table 3). The barrier accumulation rate then decreased to 58.6 $m^3/yr\ m^{-1}$ at GLc3. This compartment has shoreline data over an alongshore reach of 950 m that reveals shoreline retreat of approximately 110 m (7.3 m/yr) between 1871 and 1886 (Fig. 8b).

The Grayland Plains shoreline became more concave-seaward between 1926 and 1951 due to progradation at each end of the sub-cell and erosion occurring in the middle (Fig. 13). The volume-change rates that include the upper shoreface are similar, except in northern Grayland Plains at GLc6, where the shoreline receded 3.2 m/yr while the upper shoreface accumulated 23.5 $m^3/yr\ m^{-1}$ (Table 3).

Between 1951 and 1999, shoreline change rates along Grayland Plains alternated in trend among adjacent compartments, whereas upper shoreface and barrier volume-change rates

show a regional gradient in which the highest erosion rate occurs in the north (22.1 m^3/yr m^{-1} at GLc6) and the highest accumulation rate occurs in the south (36.6 m^3/yr m^{-1} at GLc3) (Fig. 13, Table 3). Shoreline change trends across northern to central Grayland Plains at GLc6 and GLc5 also contrast with volume-change trends. The trends in shoreline change and volume change are similar in southern Grayland Plains at GLc4 and GLc3, although at GLc3, the shoreline progradation rate was relatively low compared to the rate of upper shoreface and barrier accumulation.

3.3.3 North Beach Shoreline and Volume Changes

Similar to the late prehistoric to early historical shoreline changes at Clatsop Plains, Long Beach, and Grayland Plains, shoreline change rates along North Beach were highest near the estuary entrance and decreased with distance alongshore (Fig. 13). At southern North Beach (NBds) between 1700 and 1886 the shoreline prograded 4.8 m/yr, compared to 2.7 m/yr averaged from the two adjacent compartments to the north and 0.1 m/yr averaged from the four northernmost compartments. Within NBds, group-averages calculated between the 1700 paleoscarp and the more seaward 1860 shoreline, including the northern half of Eld Island, yield significantly higher shoreline progradation rates of 15.1 to 8.9 m/yr from south to north along 4 km of west-southwest facing shoreline. Based on the 1886 shoreline, the progradation rates for the same groups were only about half as high, ranging from 8.2 to 4.4 m/yr, indicating substantial shoreline retreat (> 19 m/yr) between 1860 and 1886.

The 1909 USACE survey shows that the shoreline along southern North Beach did not begin to prograde until after jetty construction began (Fig. 11). In fact, the NBds shoreline receded by an average of 10.1 m/yr (230 m) between 1886 and 1909, with most of the change resulting from northward retreat of the barrier within 1 km of the Grays Harbor North Jetty. As the jetty was constructed between 1908 and 1916, the shoal platform within about 2.5 km north of the North Jetty gradually shallowed to less than 2 m deep. Between 1916 and 1927 a narrow neck of land connected the jetty near the bend to the prograding barrier more than 1.5 km north, forming a shallow embayment to the east (Oyhut tidal flats). Between 1909 and 1927, the NBds shoreline prograded 78.6 m/yr. Within this reach, the group-averaged shoreline progradation rates from the jetty to 6 km northward ranged from 160.3 to 29.5 m/yr.

Shoreline change rates averaged between 1887 and 1927 reveal that the most significant progradation extended up to 11.2 km north of the North Jetty within the southern two compartments (NBds and NBc1). These compartments prograded by 29.1 and 5.2 m/yr, respectively, exceeding the shoreline progradation rates from 1700–1887 (Fig. 13). Upper shoreface and barrier accumulation rates between 1887 and 1927 were relatively high up to 16 km north of the North Jetty, and ranged from 38.5 $m^3/yr\ m^{-1}$ (above MHW only) at NBds, to 87.2 $m^3/yr\ m^{-1}$ at NBc1, and to 23.9 $m^3/yr\ m^{-1}$ at NBc2 (Table 3). Farther north, the strand plain alternated between areas of relatively minor accretion and erosion, with consistent trends between both shoreline change and volume change.

Consistent with the high accumulation volumes calculated from the 1926 and 1954 bathymetry data along southern North Beach, the shoreline prograded at relatively high rates across a distance of more than 24 km north of the Grays Harbor North Jetty between 1927 and 1950. This alongshore pattern is similar to that observed in the shoreline changes from 1887–1927, when the southern North Beach shoreline rotated toward the west-northwest. Between 1927 and 1950, shoreline progradation took the form of a 36-km alongshore gradient with a maximum rate of 13.7 m/yr at NBds and a minimum rate of 2.4 m/yr at NBc6 (Fig. 13). The two northernmost compartments lack shoreline data during the 1950s; Fig. 13 substitutes 1967 data. The upper shoreface and barrier volume-change rates correspond well to the regional shoreline change gradient (Table 3). The highest accumulation rate was 159.7 $m^3/yr\ m^{-1}$ at NBc1. NBc2 experienced a similar accumulation rate of 151.4 $m^3/yr\ m^{-1}$, indicating a northward migration of the depocenter compared to the previous interval. Farther north, the strand plain accumulated at rates ranging from 96.5 $m^3/yr\ m^{-1}$ at NBc3 to 24.2 $m^3/yr\ m^{-1}$ at NBc6. Change rates are not calculated at NBc7 and NBc8 because of insufficient data.

The compartment-averaged shoreline progradation rates between the 1950s and 1999 are nearly all less than half of those of the previous interval (Fig. 13). Averaged over 1950–1999, the shoreline progradation rates are 4.0 m/yr at NBds, then increase to 5.9 m/yr at NBc1, then decrease northward at each compartment from 4.8 m/yr at NBc2 to 0.2 m/yr at NBc5. All shoreline change rates for groups between 0.8 and 23 km north of the Grays Harbor North Jetty consistently show net progradation. The upper shoreface and barrier accumulation rates between 1954 and 1999 reveal a similar regional gradient (Table 3).

The rates of both shoreline change and volume change between NBc2 and NBc3 are more similar between 1954 and 1999 than 1927 and 1954, indicating a northward propagation of the barrier depocenter. The compartment-averaged shoreline changes along southern to central North Beach (NBds to NBc3) consistently show progradation during all periods between 1950 and 1999, whereas farther northward (NBc4 to NBc6) shoreline changes between 1950 and 1967 indicate recession (Fig. 9). The shoreline at NBc4 and NBc5 receded between 1995 and 1999, whereas the NBc7 shoreline prograded.

4.0 SUMMARY OF THE CRLC HISTORICAL EVOLUTION

The evolution of the CRLC since the late 1800s has been marked by the following:

- Large signals of shoreline change (on horizontal scales of meters to kilometers);
- Large signals of bathymetric change (on vertical scales of centimeters to meters);
- Large transfers of sand (typically on the scales of 10^6 m^3 and tens to hundreds of m^3/yr per meter alongshore).

These changes have been primarily caused by the construction of jetties at the entrances to the Columbia River (1885–1913) and Grays Harbor (1898–1916), which established new boundary conditions, modified local sediment supplies, and induced system-wide morphological responses at the decade-to-century time scale.

Long-term shoreline progradation rates across the littoral cell increased from roughly 1–2 m/yr during the late prehistoric period (1700–1860s) to roughly 5–10 m/yr during the initial decades following jetty construction. The highest late prehistoric shoreline

progradation rates occurred along the barrier spits at northern Long Beach (up to 25.8 m/yr) and southern North Beach (up to 15.1 m/yr), but significantly higher post-jetty shoreline progradation rates were also recorded at these locations (107.6 and 160.3 m/yr, respectively). From the early 1900s to present, much of the shoreline has prograded on the order of 0.4 km (3.5 m/yr), with significant spatial variability ranging from shoreline recession of 3.8 km (29.8 m/yr) at Cape Shoalwater to shoreline progradation of 4.5 km (34.7 m/yr) at Clatsop Spit. Adjacent to each of the jetties, the shoreline prograded up to 2.5 km (Long Beach), 0.5 km (Grayland Plains), and 2.3 km (North Beach). The abrupt shoreline progradation adjacent to the jetties was due mostly to onshore-directed sand flux from the flanks of the ebb-tidal deltas at the entrances to the Columbia River and Grays Harbor. After jetty construction and inlet narrowing, the flanks were no longer significantly influenced by the ebb jet. Over several decades following the initial onshore pulse of sand to the coasts adjacent to the jetties, sand was dispersed alongshore, modifying the regional shoreline position and orientation up to tens of kilometers from the jettied entrances. During the latter half of the 20th century, shoreline progradation rates in the CRLC generally slowed, and the shorelines immediately adjacent to the jetties have become either dynamically stable or have reversed in trend to recession as the morphology approaches a new equilibrium following the initial perturbation from jetty construction.

The depocenter of the ebb-tidal delta at each stabilized inlet has migrated offshore in a northwesterly direction and deepened since jetty construction. The inner deltas have roughly doubled in depth over the past century. The Columbia River inner delta has

deepened from 9.5 m in 1868 to 17.8 m in 2000. The Grays Harbor inner delta has deepened from 6.0 m in 1900 to 12.4 m in 1999. At both inlets, the outer-delta areas that accumulated sediment during and immediately after jetty construction later began to erode, and the depocenters migrated offshore. The northerly and offshore migration of the ebb-tidal deltas has increasingly separated them from Clatsop Plains and Grayland Plains. Over the century since jetty construction, the relict southern flanks of these ebb-tidal deltas have deflated by several centimeters per year. This deflation is expected to continue over the next several decades, albeit at lower rates. As the ebb-tidal deltas continue to migrate offshore over the next several decades, they will also progressively detach from Long Beach and North Beach. The expanded area of inner-delta erosion north of the inlets over the three historical intervals is evidence of this separation.

The ebb-tidal delta evolution at the MCR and the MGH had similar patterns, despite some differences in relative volume change. While both inlets experienced outer-delta deposition during the first interval (1870s–1920s), the MCR outer delta accumulated three times more than the inner delta eroded, whereas the MGH outer delta accumulated only one-third as much as the inner delta eroded. During the second interval (1920s–1950s), both outer deltas accumulated about twice as much as the inner deltas eroded. During the third interval, both outer deltas accumulated a similar amount to that eroded from the inner deltas, implying the southern flanks and shoreface were no longer supplying an abundance of sediment to the outer deltas as they did during the second interval. In total, the MCR outer delta accumulated more than twice the amount of sediment eroded from the inner delta, whereas the MGH outer delta accumulated only

slightly more sediment than eroded from the inner delta. Regardless of the relative volume differences, the outer-delta deposition zones of the first interval (1870s–1920s) were subsumed by expansion of inner-delta erosion during the third interval (1950s–1999) at both inlets.

While jetty construction has induced erosion within the inlets and inner deltas, offshore and northerly migration of the ebb-tidal delta depocenters, and deflation of the ebb-tidal delta flanks, other human interventions have also contributed to changes affecting the sediment budget. To some extent, particularly at the MCR, sand volume transfers have been mechanically enhanced through channel dredging and offshore disposal. In recent decades, offshore disposal of dredged sand from the Columbia River entrance has significantly reduced the littoral sediment budget and contributed to erosion of the inner delta and adjacent coasts. Additionally, dams and irrigation have reduced river flows and sand supply from the Columbia River—the primary source of CRLC sediment—over the historical period. From the time significant flow regulation began in 1969 (Sherwood et al., 1990) through 2008, the USACE has disposed 53.5 Mm^3 of dredged sand outside the littoral zone (Sites B and F in Fig. 4c and farther offshore) (USACE, 2009). This amount is nearly equivalent to the estimated supply of fluvial sediment to the estuary during this period (Gelfenbaum et al., 1999). At present, the balance between sand import to and export from the estuary remains unclear. The probability of significant sand export has likely decreased with the reduction in the magnitude and frequency of peak floods (Lockett, 1963).

Although massive redistribution of sand within these entrances and ebb-tidal deltas accounts for much of the historical change in sand volume of the barriers and strand plains, it does not account for all of it. At the Willapa Bay entrance, the shoreline retreated by more than 10 m/yr along both sides of this dynamic inlet within two decades of jetty construction at the adjacent inlets. Since then, the Willapa Bay entrance channel has migrated northward, completely eroding away Cape Shoalwater, the large spit that had extended from the present southern end of Grayland Plains to about 5 km into the Willapa Bay entrance (Fig. 8a,b). The Willapa Bay ebb-tidal delta has shifted northward along with the migrating entrance channel. Aside from an occurrence of a Cascadia coseismic subsidence event, the present setting offers no mechanism for restoration of Cape Shoalwater (Morton et al., 2007). Both sediment impoundment north of Grays Harbor and seaward rotation of the southern Grayland Plains shoreline have diminished the potential for southward littoral sediment transport, compared to the late 1800s, when Cape Shoalwater prograded southward.

Commensurate with shoreline changes along the barrier-plain beaches, the shoreface profile across much of the inner shelf has also adjusted. Within each sub-cell, the upper shoreface has aggraded on the order of a couple meters. The toe of the progradational sand wedge has migrated seaward on the order of a few hundred meters in each sub-cell (Fig. 14a) except Grayland Plains and the northernmost Clatsop Plains, where it has remained relatively stationary in association with shoreface rotation (Fig. 14b). Upper shoreface accumulation along Clatsop Plains and Grayland Plains is at least in part due to onshore transport of sand that has eroded from the mid- to lower shoreface (between

roughly 10 and 30 m water depth). In contrast, the southern Long Beach mid- to lower shoreface has aggraded in response to an abundant supply of sand eroded from the Clatsop Plains shoreface and dispersed from the Columbia River ebb-tidal delta.

The contemporary sediment pathways, fluxes, and volumes in the compartments that make up the system-wide sediment budget differ from those of the recent prehistoric era in a number of ways. Human interventions have enhanced the segmentation of the littoral cell, comparatively decreasing sediment-sharing between adjacent coasts. Prior to jetty construction, the adjacent coasts were co-linear and linked across the entrance by shallow ebb-tidal shoals and shore-connected platforms that were no more than 5 m deep. With jetty construction and dredging, the northern coast became offset by roughly 2 km to the west of the southern coast. The inner shoals dispersed such that the shallowest contiguous contour across the entrances is now no less than 20 m deep. The sediment from the inner deltas was jetted offshore and deposited in the outer deltas, where the main sediment pathway is driven by winter storm transport to the north. As a result, southerly sediment transport across the jettied estuary entrances that occurs primarily during fair-weather conditions in shallower water has significantly diminished.

In effect, the contemporary entrance-ebb-tidal delta subsystems function as a one-way valve for alongshore sediment transport. Large winter waves, predominantly from the southwest, induce net northward sediment transport across the ebb-tidal deltas. Fair-weather summer waves from the northwest induce southward sediment transport, but not enough to balance the northward transfer of sand from the sub-cell on the south side of

each stabilized inlet. Thus, northern Clatsop Plains and Grayland Plains have prograded to a much lesser extent than the southern ends of their respective northward counterparts, Long Beach and North Beach. Peak shoreline progradation occurring near one, if not both, ends of each sub-cell has reshaped each shoreline to a more concave configuration, corresponding to boundary conditions imposed by the jetties, proximity to local sand supplies, and alongshore gradients in net sediment transport.

Since jetty construction nearly a century ago, bathymetric change rates at the MCR and MGH have gradually decreased, and the peaks in sediment accumulation rate along the adjacent coasts have migrated away from the entrances. Exceptions to the trend of decreasing rates of change are shoreline progradation and upper shoreface accumulation along central to northern Long Beach (LBc3–LBdn) and northern North Beach (NBc7–NBc8). These two reaches show higher rates of accretion during the last interval than during previous intervals. The higher accretion rates are likely due to both the change in shoreline orientation along the southern portion of these sub-cells (which has enhanced northward sediment transport) and the increase in sediment supply associated with the one-way valve effect described above. Aside from these exceptions, the rates of accumulation and erosion have decreased, suggesting the littoral cell is approaching a new post-jetty dynamic equilibrium. Nevertheless, the relatively slow decline in change rates and the magnitude of contemporary morphological trends (Ruggiero et al., 2005) indicate that it will take at least several more decades for the regional-scale system to reach this new state.

5.0 DISCUSSION OF KEY FINDINGS

5.1 Insights from the Prehistoric Shoreline

The shoreline position inferred from the A.D. 1700 paleoscarp and the change rates calculated between the scarp line and pre-jetty shoreline suggest that coseismic subsidence truncated the barrier spits and eroded each CRLC barrier and strand plain along their entire length. At the estuary entrances, coseismic subsidence would have induced bayward sediment transport and estuary infilling as a result of increased accommodation space.

Commensurate with interseismic uplift, the spits would have rapidly prograded, separating recurved dune ridges from the shoreline by a broad coastal plain. This process would explain why shoreline progradation rates are highest along the barrier spits of each estuary entrance. High rates of spit growth would be consistent with rebound-induced export of sediment from the estuaries, which increases sediment supply to the adjacent beaches.

Shoreline change rates from the back edge of the barriers to the A.D. 1700 paleoscarp do not indicate higher accretion rates near the estuary entrances (Woxell, 1998; Peterson et al., 1999), which implies that excess barrier accretion has only been maintained during interseismic periods following sufficient rebound. The low barrier spits are subsequently truncated during each coseismic subsidence event.

Table 4 compares shoreline change rates during the late prehistoric period (prior to jetty construction) to long-term historical rates, when the response to jetty construction was dominant. The long-term historical shoreline change rates are approximately double the pre-jetty shoreline change rates since 1700.

5.2 Columbia River Sediment Supply

Analysis of the CRLC sediment budget shows that the Columbia River sediment supply has declined over the historical period due to human interventions, especially flow regulation and dredging (Sherwood et al., 1990; Gelfenbaum et al., 1999). Erosion patterns in the vicinity of the MCR suggest that the Columbia River sediment supply is insufficient to maintain the ebb-tidal shoals and adjacent coasts in their present configuration. Under these conditions, barrier stability increasingly depends on sediment supply from the shoreface. While dredged material is an important source of sediment, it is not enough to overcome the present deficit.

The balance of volume-change analysis for the MCR between 1868 and 1926 suggests that some of the sand from the entrance may have been transported into the estuary, contributing to accumulation of the flood-tidal shoals. This is an intriguing result given that river supply of sand to the estuary is estimated to be highest (4.3 Mm^3/yr) between 1878 and 1934 (Gelfenbaum et al., 1999). Further, the same study estimates that the river supply of sand to the estuary declined by a factor of 3 (from 4.3 Mm^3/yr between 1878 and 1934 to 1.4 Mm^3/yr between 1958 and 1997) as a result of flow modification by dams.

While these estimates are useful for constraining the sediment budget, the exchange of sediment between the estuary and the coast remains largely unknown. Other studies (e.g., Lockett, 1967; Morse et al., 1968; Walter et al., 1979) have suggested that sand from the littoral environment enters and potentially accumulates in the estuary. The USACE has dredged sand from the MCR and lower estuary and deposited it on the mid-shelf in water depths greater than 40 m (USACE, 1999). Between 1956 and 1983, 0.9 Mm^3/yr (25 Mm^3) of sand was disposed in deep water outside the littoral system. That amount increased to 2.5 Mm^3/yr (34.6 Mm^3) between 1984 and 1998. Because the rate of removal since 1984 has been greater than the rate of river supply of sand to the estuary, it is possible that there is presently no net supply of sand from the river to the littoral environment.

Clearly, a decreasing sediment supply from the Columbia River has implications for the entire littoral cell, yet this decline has had a smaller impact on the adjacent coasts because the ebb-tidal shoals provided a significant supply of sand over several decades following jetty construction. The present high rates of shoreline progradation along the central to northern Long Beach sub-cell and central North Beach sub-cell (Ruggiero et al., 2005) suggest that the remnant ebb-tidal shoals, the shoreface, or both continue to supply significant quantities of sand to the downdrift barriers.

5.3 Onshore Sediment Flux from the Mid- to Lower Shoreface

Historical bathymetric data show a consistent erosion pattern of the mid- to lower shoreface in water depths of approximately 10–24 m and accumulation of the upper shoreface and barrier. This pattern is accentuated along the northern portions of Clatsop Plains and Grayland Plains during all historical intervals (1870s–1920s, 1920s–1950s, and 1950s–1999); shoreface erosion along both Clatsop Plains and Grayland Plains is almost always greater than strand plain accumulation during all intervals (Table 5). Interpreting this pattern raises questions relating to: 1) why the erosion rates for the mid- to lower shoreface are higher than the accumulation rates for the upper shoreface and barrier; 2) whether the pattern could be explained by erroneous bathymetric data; 3) what process mechanisms might explain the changes; and 4) what additional research might provide further insights into the processes that drive the morphological changes.

In the case of Clatsop Plains, construction of the Columbia River South Jetty is considered to have eliminated sand supply to Clatsop Plains because net sediment transport across the lower shoreface is northward and the jetty severed southward ebb-current transport of sand to the shoreface (Hickson and Rodolf, 1951; Ballard, 1964; Byrnes and Li, 2001). Lockett (1967) suggests that the lower shoreface erosion along Clatsop Plains is related to the jetties blocking southward transport of sand from the north. Komar and Li (1991) agree with this assessment, adding that erosion south of the entrance may be due to a combination of factors, including the reflection of incident southwest storm waves, enhancing southward sediment transport.

Supporting these propositions, this study shows that large morphological changes (i.e., net sediment fluxes) between 1868 and 1926 are balanced between mid- to lower shoreface erosion, strand plain accumulation, and outer-delta accumulation. In sum, the Clatsop Plains shoal and mid- to lower shoreface provided the upper shoreface and strand plain with 74 Mm^3 (1.3 Mm^3/yr). The remaining 173.2 Mm^3 (3.0 Mm^3/yr), (i.e., 70 percent) of sediment is inferred to be have been transported to the northwest, where it accumulated in the outer delta, which gained 171.5 Mm^3 (3.0 Mm^3/yr). Buijsman et al. (2003b) conclude that to balance the accumulation of sand along Clatsop Plains, sand had to have been transported onshore from the eroding southern flank of the Columbia River ebb-tidal delta and lower shoreface during all intervals. This analysis is consistent with previous interpretations of shoreface feeding of sand to Clatsop Plains (Hickson, 1936; Hickson and Rodolf, 1951; Ballard, 1964).

The inference of onshore sediment supply from the shoreface is further supported by comparative analyses of historical shoreface profiles and vibracore data (Kaminsky et al., 2007). Vibracore data are consistent with erosion across the Clatsop Plains mid- to lower shoreface observed in the historical bathymetry data; the vibracores contain near-surface relict tidal-inlet deposits, 'old' radiocarbon ages, winnowed or lag deposits, and inferred rip-up clasts and mud clasts, each of which are indicative of an erosional surface (e.g., Liu and Zarillo, 1989; Schwab et al., 2000; Belknap et al., 2002). Near-surface sediment across the Clatsop Plains shoreface is significantly coarser (i.e., winnowed) than that from the adjacent Long Beach shoreface north of the MCR.

In the case of Grayland Plains, the Grays Harbor South Jetty has not induced significant shoreline progradation, as would be expected along a coast with net northward littoral sediment transport. In contrast, the shoreline progradation rate averaged over the entire historical period is lower next to the jetty than at any compartment along Grayland Plains (Table 4). Similar to the sediment balance at Clatsop Plains, erosion of the mid- to lower shoreface can account for the accumulation of the strand plain during the first interval (1900–1920s); the difference between the amount eroded from the shoreface and accumulated along the barrier (15.2 Mm^3) balances the accumulation of the outer delta, while the erosion of the inlet and inner delta (79.5 Mm^3) can account for the accumulation along North Beach (73.6 Mm^3). While the volume-changes balance, it is intriguing that strand plain progradation is highest in central Grayland Plains and volume-change rates there are also relatively high (up to 105 $m^3/yr\ m^{-1}$). The pattern and rates of change suggest that the shoreface was out of equilibrium on a regional scale following jetty construction. It is likely that the Grays Harbor South Jetty eliminated southward-directed tidal currents and sediment supply along Grayland Plains in such a way that the post-jetty mid-shoreface profile was too shallow for the wave-dominated energy regime, and it therefore deepened rapidly toward a new equilibrium.

From the 1920s to 1950s, the Grayland Plains shoreface and strand plain volume changes are small and nearly balance. During this time, most of the accumulation along Grayland Plains was adjacent to the MWB, and related to the northward migration of the entrance channel and shore-attached shoal. Within 1 km of the Grays Harbor South Jetty, a jetty fillet advanced 6.7 m/yr, likely associated with jetty rehabilitation between 1935 and

1940 (Buijsman et al., 2003a). Just south of the fillet, the shoreline retreated up to 5 m/yr at 3 km south of the Grays Harbor South Jetty. From that point southward the shoreline retreat rate shows a regional gradient that tapers to zero at 8 km south of the jetty, then increases to 6.2 m/yr of progradation in GLc3 (Fig. 13) and up to 8.2 m/yr of progradation (group-averaged) near the MWB. This pattern suggests a divergence in littoral alongshore sediment transport along northern Grayland Plains and a convergence in littoral transport toward southern Grayland Plains corresponding to the change in regional shoreline orientation.

From the 1950s to 1999 the Grayland Plains mid- to lower shoreface again eroded substantially, while the upper shoreface and strand plain volume-change rates show an alongshore gradient from moderately high erosion (22.1 $m^3/yr\ m^{-1}$) along northern Grayland Plains to moderately high accumulation (36.6 $m^3/yr\ m^{-1}$) near the MWB (Table 3). This trend suggests a dominance of southward littoral sediment transport during this interval, with the upper to mid-shoreface in northern Grayland Plains supplying some of the sand that accumulated along central Grayland Plains. Most of the mid- to lower shoreface erosion of 53.9 Mm^3 (1.2 Mm^3/yr) is inferred to have contributed sediment to the Grays Harbor outer-delta areas, which accumulated a total of 62.9 Mm^3 (1.4 Mm^3/yr). The morphological changes over the three intervals suggest that most of the onshore sediment flux occurred within a decade of jetty construction, after which the net changes became governed by divergences in alongshore and cross-shore sediment flux.

Additional evidence for the shoreface erosion observed in the bathymetric data includes side-scan sonar imagery, multibeam backscatter data, and surface sediment samples on the northern Grayland Plains mid-shoreface that reveal rippled scour depressions (i.e., sorted bedforms) (Twichell and Cross, 2001; Ferrini and Flood, 2005). Onshore from these rippled scour depressions, prograded beach deposits contain relict granules and pebbles, implying their onshore transport along with Columbia River sand. Ruggiero et al. (2005) show that the northern Grayland Plains beach is composed of the coarsest sediment of any of the CRLC beaches. While the mid-beach sediments throughout the CRLC show a mean grain size of 0.18 mm, that of the northern Grayland Plains mid-beach ranges from 0.60 to 0.71 mm. The coarse sand, granules, and gravel contributing to this beach most likely have been derived from reworking and landward transport of glacial outwash (Venkatarathnam and McManus, 1973) on the mid- to lower shoreface. Vibracores collected on the mid-shoreface of Grayland Plains recovered near-surface lag deposits (Kaminsky and Ferland, 2003).

Based on the available morphological change data, the sediment budget does not balance for any interval. Analysis of Buijsman et al. (2003b) shows that no balance can be achieved by either integrating over all volume-change areas (which exclude much of the shoreface), or considering all datum adjustments, reasonable estimates of Columbia River sediment supply, and modeled sediment transport fluxes. Between the 1860s and 1920s the sediment budget yields approximately 4 Mm^3/yr more erosion than accumulation. From the 1920s to 1950s the sediment budget yields approximately 12 Mm^3/yr more accumulation than erosion. From the 1950s to 2000 the sediment budget yields

approximately 4 Mm^3/yr more accumulation than erosion. The conclusion of Buijsman et al. (2003b) is that higher sediment input from either the estuaries or the shoreface, or both, must have occurred during the periods of excess accumulation. Based on an integrated sediment budget analysis and the available data of the estuary entrances, Kaminsky et al. (2001) conclude that shoreface sediment supply is the most reasonable explanation to account for the excess sediment accumulation from the 1950s to 2000.

Relatively few studies have conclusively documented shoreface sediment supply to beaches (Cowell et al., 2001). Most estimates of net onshore sediment transport are derived from late-Holocene prograded barriers, which lacked a significant fluvial source (Roy and Thom, 1981; Roy et al., 1994; Short, 2003). A few studies have documented shoreface supply of sand to beaches from decadal-scale shoreface profile and bathymetric data (Cooper and Navas, 2004; Hinton and Nicholls, 2007). It is inherently difficult to infer net shoreface sediment transport from either process measurements or long-term morphological changes, as large fluctuations in sediment motion and small transport residuals often characterize the sediment transport environment. In one of the few cases where this phenomenon has been quantitatively confirmed, Wright et al. (1994) document 18 cm of shoreface accumulation in 14 m water depth on the Duck, North Carolina shoreface resulting from onshore sediment transport due to a mild storm event in October 1992.

Wave asymmetry and wave-driven residual flow in the bottom boundary layer are principal mechanisms for onshore sediment transport from the lower shoreface (Bowen,

1980; Stive and de Vriend, 1995). Wind-driven currents and upwelling may enhance the effect of wave asymmetry in transporting sediment in the onshore direction (Niedoroda et al., 1984). Stive et al. (1991) hypothesize that smaller storm events are effective in transporting sediment onshore from the lower to upper shoreface, which is consistent with the observations of Wright et al. (1994). Parkinson (1991) hypothesizes that low-steepness swell is primarily responsible for net onshore sand transport.

Rates of shoreface sand supply to beaches are typically on the order of 1–10 $m^3/yr\ m^{-1}$, a volume equivalent to shoreface change of a few grain diameters per year (Cowell et al., 2001). For example, on interannual time scales on the Skallingen shoreface along the southwestern coast of the Danish North Sea, Aagaard et al. (2004) estimate the mean onshore sediment supply from the shoreface to be 6–7.5 $m^3/yr\ m^{-1}$. On millennial time scales, Beets et al. (1992) estimate that at least half of the sediment comprising the progradational strand plains of the central Netherlands coast was derived from the lower shoreface of the North Sea at a rate of approximately 4.6 $m^3/yr\ m^{-1}$. At Moruya Beach (a prograded strand plain in an embayment that precludes a littoral sediment supply) in New South Wales, Australia, radiocarbon dating suggests a declining rate of shoreface sand supply from approximately 7 $m^3/yr\ m^{-1}$ at 6000 BP to 3.3 $m^3/yr\ m^{-1}$ at present (Thom, 1984). Short (2003) estimates that Holocene rates of onshore sediment transport to the Australian coast range from a low of 0.1 $m^3/yr\ m^{-1}$ in the tide-dominated northwest coast to a high of 11.1 $m^3/yr\ m^{-1}$ along the wave-dominated sand islands of southeast Queensland and parts of the exposed southern Australian coast.

Shoreface sand supply rates in the CRLC are inferred to be significantly higher, with values up to 121.6 $m^3/yr\ m^{-1}$ along central Clatsop Plains from 1926 to 1958 (Table 3). Of course, such extreme rates represent significant disequilibrium response to jetty construction rather than 'naturally occurring' behaviour (Kaminsky et al., 2007). Along open coast reaches of Long Beach and North Beach, Kaminsky et al. (2001) estimate shoreface sand supply rates of 31.4 and 27.3 $m^3/yr\ m^{-1}$, respectively, based on sediment budget analysis.

In the CRLC, a number of factors may contribute to mid- to lower shoreface erosion rates that are larger than the rates of upper shoreface and barrier accumulation. Erosion of the northern Clatsop Plains mid- to lower shoreface has been especially high where the morphological profile was found to be significantly out-of-equilibrium (too shallow) relative to the energy regime (Kaminsky et al., 2007). Two other factors may include an increase in wave heights in the Pacific Northwest (Allan and Komar, 2000, 2006; Graham and Diaz, 2001) and a decrease in sediment supply from the Columbia River (Gelfenbaum et al., 1999). A more vigorous wave climate would be expected to enhance shoreface sediment transport, while a reduction in sediment supply would affect the morphological equilibrium (Swift and Thorne, 1991).

Process measurements in the CRLC indicate that shoreface sediment transport is dominated by wave processes (Moritz et al., 1999; Lacy et al., 2005; Moritz et al., 2006; Sherwood et al., 2006). For example, during spring and summer months with wave heights less than 2 m, bottom orbital velocities up to 100 cm/s (median of 45 cm/s)

dominate over near-bottom currents of up to 48 cm/s (median of 13 cm/s) in 9-m water depth (Lacy et al., 2005; Sherwood et al., 2006). Wave orbital velocities increase shoreward, nearly doubling between 24 and 13 m water depth (Landerman et al., 2004). Asymmetric oscillatory motion augmented by upwelling circulation promotes onshore sand transport during these summer conditions (Osborne et al., 2002, Sherwood et al., 2006). Although winter suspended load transport across the lower shoreface is generally northward and offshore, net bedload transport has been found to be onshore even during winter storm conditions, including downwelling circulation and offshore Ekman transport (Sherwood et al., 2001). Process-response studies aimed at understanding the relationship between hydrodynamics, sediment transport, and morphology change suggest that cross-shore sediment transport processes are more important than alongshore sediment transport processes in simulating seasonal onshore bar migration and beach progradation in the CRLC (Ruggiero et al., 2003b; Walstra et al., 2005). Morphology-change measurements show a strongly cross-shore dominated signal of erosion in water depths > 4 m and beach accumulation in water depths < 4 m, with model simulations indicating substantial feeding of sediment from water depths > 8 m (Ruggiero et al., 2003b).

The implication for CRLC evolution is that the shoreface has provided a significant supply of sand to the barriers as a result of disequilibrium. The rate of onshore sediment supply from remnant ebb-tidal shoals and the adjacent shoreface is expected to decrease over time, but rigorous quantitative analysis has yet to be completed. Since shoreline change predictions depend on accurate estimates of sediment supply from the shoreface

(Kaminsky et al., 2001; Buijsman et al., 2001; Ruggiero et al., this issue), the efficacy of feeding dredged sand to the littoral system by placing it across the mid- to lower shoreface remains a key question requiring additional research.

5.4 Bi-directional Shoreface Sediment Transport

The mid- to lower shoreface sediment fluxes discussed above indicate a divergence in sediment transport whereby sediment appears to be transferred from the mid- to lower shoreface onshore and southward to accumulate along Clatsop Plains and Grayland Plains, as well as northward to accumulate in the outer deltas. Clearly, the predominance of waves from the west-southwest during winter and west-northwest during summer (Ruggiero et al., 1997) contributes to the bi-directional sediment transport that is inferred from the volume-change analysis. From the results of shoreline modeling and morphodynamic analysis Kaminsky et al. (2001) conclude that the net sediment transport along the upper shoreface and littoral zone is presently directed away from the jettied estuary entrance—a significant difference from the pre-jetty configuration. In contrast, the net regional transport of sand along the lower shoreface appears to be both northerly and onshore over decade-to-century time scales throughout the entire littoral cell, based on barrier accumulation rates (Table 3). Fine sediments have a net northerly and offshore flow (Nittrouer and Sternberg, 1981; Kachel and Smith, 1989). Importantly, resolving net cross-shore sediment transport must account for grain sorting, given the available evidence of barrier accumulation of sand and mid-shelf accumulation of fine sediments (Nittrouer and Sternberg, 1981).

The divergence in net sediment transport direction is most evident along Clatsop Plains, and to a lesser degree, along Grayland Plains. Along Clatsop Plains, onshore and southerly sediment transport is inferred from the pattern of mid- to lower shoreface erosion and upper-shoreface accumulation; with increasing distance from the MCR, the mid- to lower-shoreface erosion rates decrease, while the upper shoreface accumulation rates increase. However, since the amount of erosion across the mid- to lower shoreface is greater than the accumulation onshore, significant northward sediment transport from the lower shoreface toward the outer delta is also inferred. In contrast, southward sediment transport is not inferred from the pattern of accumulation along Long Beach between the 1920s and 1950s (high erosion in the north and high accumulation in the south). Morphological changes around the MCR ebb-tidal delta strongly indicate net northward sediment flux. The accumulation along southern Long Beach is inferred to be the result of an abundant sediment supply resulting from erosion of the inlet and inner delta, and northward and landward dispersal of sand from these sources. The northward migration of the barrier depocenter over time supports this inference. While the bathymetric data do not exist to determine conclusively, shoreline recession at Leadbetter Point and northern Long Beach between the 1920s and 1950s may be associated with changes in the shoals and channels at the MWB. Historical condition surveys show the re-development of a southern channel in 1945 that ran southward along the shoreline until 1949, after which it migrated northward (Hands, 2000b). The dominance of northward sediment transport is supported by regional gradients of decreasing sediment accumulation and grain size across the inner to mid-shelf (Nittrouer and Sternberg, 1981;

Twichell and Cross, 2001) and decreasing grain settling velocities (Li and Komar, 1992) and grain size (Ruggiero et al., 2005) along the beaches with distance north from the MCR.

The North Beach sediment accumulation patterns are similar to those of Long Beach, with a regional alongshore gradient of decreasing accumulation rates (and decreasing grain size) with distance north of the MGH. While the Grays Harbor North Jetty likely captured sand transported southward alongshore by nearshore currents (Osborne et al., 2002; Buijsman et al., 2003a), the regional gradient in volume change and shoreline progradation northward from the MGH can be explained only by northward sediment dispersal from the MGH and by sediment bypassing the inlet from the Grayland Plains shoreface. The alongshore dispersal of sediment is consistent with the change in shoreline orientation along southern North Beach from pre-jetty to 1926, when the shoreline effectively rotated toward the west-northwest. This rotated shoreline likely enhanced northward sediment transport due to the more acute angle relative to incident winter storm waves coming predominantly from the southwest. The northward dispersal of sediment is shown by the northward migration of the barrier depocenter over the historical period. The lack of significant sand deposits along the shelf and strand plain of northern North Beach (Twichell et al., this issue; Vanderburgh et al., this issue) implies that sediment accumulation along southern North Beach can only be supported by net northward sediment transport. Most of the lower shoreface along North Beach is composed of glacial outwash or bedrock (Twichell and Cross, 2001) that is largely devoid of Columbia River sediment. Finally, the narrow strand plain along northern

North Beach exhibits the finest grain sizes and the lowest sloping beaches within the CRLC (Ruggiero et al., 2005), indicating net northward transport of littoral sand.

6.0 CONCLUSIONS AND FUTURE DIRECTIONS

This study has clarified that jetties had a first-order effect on the historical coastal evolution of the CRLC, while the effect of dam construction and flow regulation appears to have been more subtle and gradual, and currently remains subsumed within the effects of the jetties. The jetties significantly disturbed the equilibrium of the entire coastal system, causing a local response over short time scales and a regional response over long time scales. The anthropogenic reduction in sediment supply from the Columbia River over the historical period implies that the system will continue to evolve toward a new dynamic equilibrium. This equilibrium will become more evident as the morphological effect of the jetties wanes. As the coastal sediment supply from the river, inlets, shoals, and shoreface continues to decrease, strategic management of material dredged from the inlets and estuaries will become increasingly important.

The analyses of historical shoreline and bathymetric data, spanning a time prior to human influence to a century following the major intervention of jetty construction, has provided a number of insights into the temporal and spatial scales of coastal evolution in the CRLC. Due in part to the magnitude of the morphological changes, regional-scale patterns and trends are apparent at decadal time scales. Some of the results challenge traditional concepts and understanding of coastal dynamics.

The data provide ample evidence of cross-shore feeding from the shoreface to the barriers. Many lines of evidence within the CRLC point to a significant volume of sediment being transferred onshore from the lower to upper shoreface over time scales of decades. The CRLC may be a relatively rare example where this process manifests on these time scales. Moreover, the CRLC data demonstrate the morphological coupling between the shoreface and the barriers quite incontrovertibly.

The large change signals in the CRLC offer an ideal setting to test both process-based and behaviour-oriented models. The observed morphologic linkages between the inlets, ebb-tidal deltas, shoreface, and barriers provide the basis for advancing data-models (Cowell et al., 2003b) to investigate system responses to other perturbations. For example, the effect of sea-level rise on coastal evolution could be evaluated using an ASMITA approach (Aggregated Scale Morphological Interaction between a Tidal basin and the Adjacent coast; Stive et al., 1998) to better understand the interactions between the coast and the estuaries. Such behaviour-oriented approaches could be combined with process-based approaches (e.g., Gelfenbaum et al., 2003) to better resolve the cascade hierarchy of coastal morphodynamics.

The use of a regional paleoshoreline to derive precise shoreline change trends presents a rare opportunity to explore coastal response to a subduction zone earthquake event, and gain insight into the state and evolution of the coast long before the historical record and significant human influence. The contrast between patterns and rates of change during

the late prehistoric period and those of the post-jetty period is pronounced. The coastal response to human intervention manifests over a spatial scale of tens of kilometers and a temporal scale of over a century.

The data presented in this paper provides an opportunity to develop and test model hindcasts and forecasts using a variety of techniques (e.g., Ruggiero et al., this issue). Clearly, predictions of coastal change depend on accurate estimates of sediment supply, transport potential, net transport pathways, and morphological equilibriums. Quantitative assessments of these processes will be necessarily derived from a detailed understanding of historical coastal evolution.

7.0 ACKNOWLEDGEMENTS

The authors would like to recognize and thank several colleagues for their contributions to this paper. Christopher Sherwood and Ann Gibbs (USGS), and Jerry Franklin (Washington Department of Ecology) assisted with the development of the regional sediment budget analysis of the CRLC. Hans Moritz (USACE, Portland District), Eric Nelson (USACE, Seattle District), and Mark Byrnes (Applied Coastal Research and Engineering, Inc.) provided historical survey data. David McKinnie and Gregory Fromm (NOAA, NOS and NGS) assisted with the acquisition of historical T-sheets and the 1995 aerial photography. Richard Daniels and Robert Huxford (formerly of the Washington Department of Ecology) assisted with the derivation of historical shorelines. Curt Peterson (Portland State University) provided the paleoscarp data. Candice Holcombe

and Terry Swanson (Washington Department of Ecology) assisted with editing drafts of the manuscript. Mark Byrnes and José Jiménez provided helpful scientific reviews of the submitted manuscript. This work was performed as a contribution to the Southwest Washington Coastal Erosion Study, co-funded and directed by the Washington State Department of Ecology and the USGS.

8.0 REFERENCES

Aagaard, T., Davidson-Arnott, R., Greenwood, B., Nielsen, J., 2004. Sediment supply from shoreface to dunes: linking sediment transport measurements and long-term morphological evolution, *Geomorphology*, 60, 205–224.

Allan, J.C., Komar, P.D., 2000. Are ocean wave heights increasing in the eastern North Pacific?, *EOS, Transactions American Geophysical Union*, 81 (47), 561, 566–567.

Allan, J.C., Komar, P.D., 2002. Extreme storms in the Pacific Northwest coast during the 1997–98 El Niño and 1998–99 La Niña, *Journal of Coastal Research*, 18 (1), 175–193.

Allan, J.C., Komar, P.D., 2006. Climate controls on US West Coast erosion processes, *Journal of Coastal Research*, 22, 511–529.

Atwater, B.F., 1996. Coastal evidence for great earthquakes in western Washington, in: Rogers, A.M., Walsh, T.J., Kockelman, W.J., Priest, G.R. (Eds.), Assessing Earthquake Hazards and Reducing Risk in the Pacific Northwest, Vol. 1, U.S. Geological Survey Professional Paper 1560, pp. 77–90.

Atwater, B. F., Hemphill-Haley, E., 1997. Recurrence intervals for great earthquakes of the past 3,500 years at northeastern Willapa Bay, Washington, U.S. Geological

Survey Professional Paper 1576, U.S. Government Printing Office, Washington, 108 pp.

Atwater, B.F., Musumi-Rokkaku, S., Satake, K., Tsuji, Y., Ueda, K., Yamaguchi, D.K., 2005. The orphan tsunami of 1700; Japanese clues to a parent earthquake in North America, U.S. Geological Survey Professional Paper 1707, published in association with University of Washington Press, Seattle, 133 pp.

Ballard, R.L., 1964. Distribution of beach sediment near the Columbia River, University of Washington, Department of Oceanography, Technical Report 98, 82 pp.

Beets, D.J., van der Valk, L., Stive, M.J.F., 1992. Holocene evolution of the coast of Holland, *Marine Geology*, 103, 423–443.

Belknap, D.F., Kelley, J.T., Gontz, A.M., 2002. Evolution of the glaciated shelf and coastline of the northern Gulf of Maine, USA, *Journal of Coastal Research*, SI 36, 37–55.

Bowen, A.J., 1980. Simple models of nearshore sedimentation, beach profiles and longshore bars, in: McCann, S.B. (Ed.), *The Coastline of Canada*, Geological Survey of Canada Paper 80-10, 1–11.

Boyd, R.T., 1990. Demographic History, 1774–1874, in: Suttles, W. (Ed.), Handbook of North American Indians, Vol. 7: Northwest Coast, pp. 135–148. Smithsonian Institution Press, Washington, DC.

Buijsman, M.C., Kaminsky, G.M., Gelfenbaum, G., 2003a. Shoreline change associated with jetty construction, deterioration, and rehabilitation at Grays Harbor, Washington, *Shore & Beach*, 71 (1), 15–22.

Buijsman, M.C., Ruggiero, P., Kaminsky, G.M., 2001. Sensitivity of shoreline change predictions to wave climate variability along the southwest Washington coast, USA, *Proceedings of Coastal Dynamics '01*, ASCE, 617–626.

Buijsman, M.C., Sherwood, C.R., Gibbs, A.E., Gelfenbaum, G., Kaminsky, G.M., Ruggiero, P., Franklin, J., 2003b. Regional sediment budget of the Columbia River littoral cell, USA: Analysis of bathymetric- and topographic-volume change, *U.S. Geological Survey Open File Report* 02-281, 140 pp.

Burch, T.L., Sherwood, C.R., 1992. Historical Bathymetric Changes Near the Entrance to Grays Harbor, Washington. Batelle/Marine Sciences Laboratory Sequim, Washington.

Byrnes, M.R., Baker, J.L., 2003. Chapter 3: Inlet and Nearshore Morphodynamics, in: Kraus, N.C., Arden, H.T. (Eds.), North Jetty Performance and Entrance Navigation Channel Maintenance, Grays Harbor, Washington, Volume I: Main Text. ERDC/CHL TR-03-12, Coastal and Hydraulics Laboratory, U.S. Army Engineer Research and Development Center, Vicksburg, MS, 67–136.

Byrnes, M.R., Li, F., 2001. Regional Analysis of Sediment Transport and Dredged Material Dispersal Patterns, Columbia River Mouth, Washington/Oregon, and Adjacent Shores, Final Report to the USACE, Coastal and Hydraulics Laboratory, Vicksburg, MS, 49 pp.

Clemens, K.E., Komar, P.D., 1988. Oregon beach-sand compositions produced by the mixing of sediments under a transgressing sea, *Journal of Sedimentary Petrology*, 58 (3), 519–529.

Cooper, J.A.G., Navas, F., 2004. Natural bathymetric change as a control on century-scale shoreline behavior, *Geology*, 32 (6), 513–516.

Cooper, W.S., 1958. Coastal Sand Dunes of Oregon and Washington. Geologic Society of America Memoir 72, New York, 169 pp.

Cowell, P.J., Hanslow, D.J., Meleo, J.F. 1999. The Shoreface, in: Short, A.D. (Ed.), Handbook of Beach and Shoreface Morphodynamics, John Wiley & Sons Ltd., pp. 39–71.

Cowell, P.J., Stive, M.J.F., Niedoroda, A.W., de Vriend, H.J., Swift, D.J.P., Kaminsky, G.M., Capobianco, M., 2003a. The coastal-tract (Part 1): A conceptual approach to aggregated modeling of low-order coastal change, *Journal of Coastal Research*, 19 (4), 812–827.

Cowell, P.J., Stive, M.J.F., Niedoroda, A.W., Swift, D.J.P., de Vriend, H.J., Buijsman, M.C., Nicholls, R.J., Roy, P.S., Kaminsky, G.M., Cleveringa, J., Reed, C.W., de Boer, P.L., 2003b. The coastal-tract (Part 2): Applications of aggregated modeling to lower-order coastal change, *Journal of Coastal Research*, 19 (4), 828–848.

Cowell, P.J., Stive, M.J.F., Roy, P.S., Kaminsky, G.M., Buijsman, M.C., Thom, B.G., Wright, L.D., 2001. Shoreface sand supply to beaches, *Proceedings of the 27th International Conference on Coastal Engineering*, 2495–2508.

Creager, J.S., Sternberg, R.W., 1972. Specific problems in understanding bottom sediment distribution and dispersal on the continental shelf, in: Swift, D. J. P., Duane, D.B., Pilkey, O.H. (Eds.), Shelf Sediment Transport, Dowden, Hutchinson and Ross, Stroudsburg, pp. 347–362.

Crowell, M., Leatherman, S.P., Buckley, M.K., 1991. Historical shoreline change: error analysis and mapping accuracy, *Journal of Coastal Research*, 7 (3), 839–852.

Doyle, D.L., 1996. Beach Response to Subsidence Following a Cascadia Subduction Zone Earthquake along the Washington-Oregon Coast, M.S. thesis, Portland State University, Portland, Oregon, 113 pp.

Ferrini, V.L., Flood, R.D., 2005. A comparison of rippled scour depressions identified with multibeam sonar: evidence of sediment transport in inner shelf environments, *Continental Shelf Research*, 25, 1979–1995.

Galster, R.W., 2005. Human influence on the Columbia River littoral cell, in: Ehlen, J., Haneberg, W.C., Larson, R.A. (Eds.), Humans as Geologic Agents: Boulder, Colorado, Geological Society of America Reviews in Engineering Geology, XVI, 67–77.

Gelfenbaum, G., Buijsman, M.C., Sherwood, C.R., Moritz, H.R., Gibbs, A.E., 2001. Coastal evolution and sediment budget at the mouth of the Columbia River, USA, *Proceedings of Coastal Dynamics '01*, 818–827.

Gelfenbaum, G., Roelvink, J.A., Meis, M., Buijsman, M., Ruggiero, P., 2003. Process-based morphological modeling of Grays Harbor inlet at decadal timescales, *Proceeding of Coastal Sediments '03*, East Meets West Productions, CD-ROM, 13 pp.

Gelfenbaum, G., Sherwood, C.R., Peterson, C.D., Kaminsky, G.M., Buijsman, M., Twichell, D.C., Ruggiero, P., Gibbs, A.E., Reed, C., 1999. The Columbia River littoral cell: a sediment budget overview, *Proceedings of Coastal Sediments '99*, 1660–1675.

Gibbs, A., Gelfenbaum, G., 1999. Bathymetric change off the Washington-Oregon coast, *Proceedings of Coastal Sediments '99*, 1627–1642.

Graham, N.E., Diaz, H.F., 2001. Evidence for intensification of North Pacific winter cyclones since 1948, Bulletin of the American Meteorological Society, 82, 1869–1893.

Gross, M.G., Morse, B.-A., Barnes, C.A., 1969. Movement of near-bottom waters on the continental shelf off the northwestern United States, *Journal of Geophysical Research*, 74 (28), 7044–7047.

Hands, E.B., 2000a. Geomorphology, in: Kraus, N.C., (Ed.), Study of navigation channel feasibility, Willapa Bay, Washington: U.S. Army Corps of Engineers Engineering Research and Development Center ERDC/CHL TR-00-6, pp. 3-1–3-45.

Hands, E.B., 2000b. Historical Charts, in: Kraus, N.C. (Ed.), Study of navigation channel feasibility, Willapa Bay, Washington: U.S. Army Corps of Engineers Engineering Research and Development Center ERDC/CHL TR-00-6, pp. A-1–A-66.

Harlett, J.C., Kulm, L.D., 1973. Suspended sediment transport on the northern Oregon continental shelf, *Geological Society of America Bulletin*, 84, 3815–3826.

Harris, C.K., Wiberg, P., 2002. Across-shelf sediment transport: interactions between suspended sediment and bed sediment, *Journal of Geophysical Research*, 107 (C1), 10.1029/2000JC000634.

Hickey, B.M., Banas, N.S., 2003. Oceanography of the U.S. Pacific Northwest Coastal Ocean and Estuaries with Application to Coastal Ecology, *Estuaries*, 26 (4B), 1010–1031.

Hickey, B., Geier, S., Kachel, N., MacFadyen, A., 2005. A bi-directional river plume: The Columbia in summer, *Continental Shelf Research*, 25, 1631–1656.

Hickson, R.E., 1922. Changes at the mouth of the Columbia River 1903 to 1921, *Journal of the Society of American Military Engineers*, 14 (76), 211–215, 257–258.

Hickson, R.E., 1936. Beach erosion at the mouth of the Columbia River, Shore and Beach, 4 (4), 147–150.

Hickson, R.E., Rodolf, F.W., 1951. History of Columbia River jetties, *Proceedings of the First Conference on Coastal Engineering*, 283–298.

Hinton, C.L., Nicholls, R.J., 2007. Shoreface morphodynamics along the Holland coast, in: Balson, P.S., Collins, M.B. (Eds.), Coastal and Shelf Sediment Transport, Geological Society of London, Special Publications, 274, 93–101.

Jol, H.M., Smith, D.G., Meyers, R.A., 1996. Digital Ground Penetrating Radar (GPR): An improved and very effective geophysical tool for studying modern coastal barriers (examples for the Atlantic, Gulf and Pacific coasts, USA), *Journal of Coastal Research*, 12 (4), 960–968.

Kachel, N.B., Smith, J.D., 1986. Geological impact of sediment transporting events on the Washington continental shelf, in: Knight, R.J., McLean, J.R. (Eds.), Shelf Sands and Sandstones, Canadian Society of Petroleum Geologists, Memoir 11, pp. 145–162.

Kachel, N.B., Smith, J.D., 1989. Sediment transport and deposition on the Washington continental shelf, in: Landry, M.R., Hickey, B.M. (Eds.), Coastal Oceanography of Washington and Oregon, 47, Elsevier, pp. 287–348.

Kaminsky, G.M., Daniels, R.C., Huxford, R., McCandless, D., Ruggiero, P., 1999a. Mapping erosion hazards in Pacific County, Washington, *Journal of Coastal Research*, SI28, 158–170.

Kaminsky, G.M., Buijsman, M., Gelfenbaum, G., Ruggiero, P., Jol, H.M., Gibbs, A.E., Peterson, C.D., 1999b. Synthesizing geological observations and processes-response data for modeling coastal change at management scale, *Proceedings of Coastal Sediments '99*, 1660–1675.

Kaminsky, G.M., Buijsman, M.C., Ruggiero, P., 2001. Predicting shoreline change at decadal scale in the Pacific Northwest, USA, *Proceedings of the 27th International Conference on Coastal Engineering*, 2400–2413.

Kaminsky, G.M., Ferland, M.A., 2003. Assessing the connections between the inner shelf and the evolution of Pacific Northwest barriers through vibracoring, *Proceedings of Coastal Sediments '03*, East Meets West Productions, CD-ROM, 12 pp.

Kaminsky, G.M., Ferland, M.A., Cowell, P.J., Moritz, H.R., Ruggiero, P., 2007. Shoreface response to sediment deficit, *Proceedings of Coastal Sediments '07,* 633–646.

Komar, P.D., Li, M.Z., 1991. Beach placers at the mouth of the Columbia River, Oregon and Washington, *Marine Mining*, 10 (2), 171–187.

Lacy, J.R., Sherwood, C.R., Wilson, D.J., Chisholm, T.A., Gelfenbaum, G.R., 2005. Estimating hydrodynamic roughness in a wave-dominated environment with a high resolution acoustic Doppler profiler, *Journal of Geophysical Research*, 110 (C06014), DOI 10.1029/2003JC001814.

Landerman, L.A., Sherwood, C.R., Gelfenbaum, G., Lacy, J., Ruggiero, P., Wilson, D., Chisholm, T., Kurrus, K., 2004. Grays Harbor Sediment Transport Experiment Spring 2001—Data Report, U.S. Geological Survey Data Series Report 98.

Li, M.Z., Komar, P.D., 1992. Longshore grain sorting and beach placer formation adjacent to the Columbia River, *Journal of Sedimentary Petrology*, 62 (3), 429–441.

Liu, J.T., Zarillo, G.A., 1989. Distribution of grain sizes across a transgressive shoreface, *Marine Geology*, 87, 121–136.

Lockett, J.B., 1959. Interim consideration of the Columbia River entrance, Paper 1902, *Proceedings of the American Society of Civil Engineers, Journal of the Hydraulics Division,* 85, HY-1, 17–40.

Lockett, J.B., 1963. Phenomena affecting improvement of the lower Columbia Estuary and Entrance, *Proceedings of the Eighth Conference on Coastal Engineering*, Council on Wave Research, and Engineering Foundation, 695–755.

Lockett, J.B., 1967. Sediment transport and diffusion: Columbia estuary and entrance, *Journal of the Waterways and Harbor Division, American Society of Civil Engineers*, WW4, 167–175.

Ludwin, R.S., Dennis, R., Carver, D., McMillan, A.D., Losey, R., Clague, J., Jonientz-Trisler, C., Bowechop, J., Wray, J., James, K., 2005. Dating the 1700 Cascadia Earthquake: Great Coastal Earthquakes in Native Stories, Seismological Research Letters, 76 (2), 140–148.

Meyers, R.A., Smith, D.G., Jol, H.M., Peterson, C.R., 1996. Evidence for eight great earthquake subsidence events detected with ground-penetrating radar, Willapa barrier, Washington, *Geology*, 24, 99–102.

Moore, L.J., 2000. Shoreline mapping techniques, *Journal of Coastal Research*, 16 (1), 111–124.

Moritz, H.R., Gelfenbaum, G.R., Kraus, N.C., 2006. Observations of cross shore infragravity energy and related pulsating bottom currents, *Proceedings of the 30th International Conference on Coastal Engineering*, 1097–1109.

Moritz, H.R., Kraus, N.C., Hands, E.B., Slocum, D.B., 1999. Correlating oceanographic processes with seabed change, mouth of the Columbia River, USA, *Proceedings of Coastal Sediments '99*, 1643–1659.

Moritz, H.R., Moritz, H.P., Hays, J.R., Sumerell, H.R., 2003. 100-years of shoal evolution at the Mouth of the Columbia River: Impacts on channel, structures, and shorelines, *Proceedings of Coastal Sediments '03*, East Meets West Productions, CD-ROM, 14 pp.

Morse, B.A., Gross, M.G., Barnes, C.A., 1968. Movement of seabed drifters near the Columbia River, *Journal of Waterways and Harbors*, ASCE, 94, WW1, 91–103.

Morton, R.A., Clifton, H.E., Buster, N.A., Peterson, R.L., Gelfenbaum, G., 2007. Forcing of large-scale cycles of coastal change at the entrance to Willapa Bay, Washington, *Marine Geology*, 246, 24–41.

Nicholls, R.J., Birkemeier, W.A., Guan-hong, L., 1998. Evaluation of depth of closure using data from Duck, NC, USA, *Marine Geology*, 148, 179-201.

Niedoroda, A.W., Swift, D.J.P. 1991. Shoreface Processes, in: Herbich, J.B. (Ed.), Handbook of Coastal and Ocean Engineering, Gulf Publishing Company, Houston, pp. 736–769.

Niedoroda, A.W., Swift, D.J.P., Hopkins, T.S., Mean-Ma, C., 1984. Shoreface morphodynamics on wave-dominated coasts, *Marine Geology*, 60, 331–354.

Nittrouer, C.A., Sternberg, R.W., 1981. The formation of sedimentary strata in an allochthonous shelf environment: The Washington continental shelf, *Marine Geology*, 42, 201–232.

Osborne, P.D., Hericks, D.B., Kraus, N.C., Parry, R.M., 2002. Wide-area measurements of sediment transport at a large inlet, Grays Harbor, Washington, *Proceedings of the 28th International Conference on Coastal Engineering*, 3053–3064.

Parkinson, R.W., 1991. Geological evidence of net onshore sand transport throughout the Holocene marine transgression, southwest Florida, *Marine Geology*, 96, 269–277.

Peterson, C.D., Doyle, D.L., Barnett, E.T., 2000. Coastal flooding and beach retreat from coseismic subsidence in the central Cascadia margin, USA, *Environmental & Engineering Geoscience*, VI (3), 255–269.

Peterson, C.D., Gelfenbaum, G., Jol, H.M., Phipps, J.B., Reckendorf, F., Twichell, D.C., Vanderburgh, S., Woxell, L., 1999. Great Earthquakes, Abundant Sand, and High Wave Energy in the Columbia Cell, USA, *Proceedings of Coastal Sediments '99*, 1676–1691.

Peterson, C.D., Vanderburgh, S., Roberts, M.C., Jol, H.M., Phipps, J., and Twichell, D.C., this issue (a). Composition, age, and depositional rates of shoreface deposits under barriers and beach plains of the Columbia River littoral cell, USA, Marine Geology.

Peterson, C.D., Jol, H.M., Vanderburgh, S., Phipps, J., Percy, D., Gelfenbaum, G., this issue (b). Dating of late Holocene shoreline positions by regional correlation of coseismic retreat events in the Columbia River littoral cell, Marine Geology.

Phipps, J.B., 1990. Coastal Accretion and Erosion in Southwest Washington, 1977-1987, Shorelands and Coastal Zone Management Program, Washington State Department of Ecology, Olympia, WA, WDOE 90-21, 40 pp.

Phipps, J.B., Smith, J.M., 1978. Pacific Ocean Beach Erosion and Accretion Report, Washington State Department of Ecology, Olympia, 75 pp.

Roy, P.S., Cowell, P.J., Ferland, M.A., Thom, B.G., 1994. Wave Dominated Coasts, in: Carter, R.W.G., Woodroffe, C.D. (Eds.), Coastal Evolution: Late Quaternary Shoreline Morphodynamics, Cambridge University Press, 121–186.

Roy, P.S., Thom, B.G. 1981. Late Quaternary marine deposition in New South Wales and southern Queensland – an evolutionary model, *Journal of Geology Society of Australia*, 28, 471–489.

Ruggiero, P., Gelfenbaum, G., Sherwood, C.R., Lacy, J., Buijsman, M.C., 2003b. Linking nearshore processes and morphology measurements to understand large scale coastal change, *Proceedings of Coastal Sediments '03*, East Meets West Productions, CD-ROM, 13 pp.

Ruggiero, P., Holman, R.A., Beach, R.A., 2004. Wave runup on a high-energy dissipative beach, *Journal of Geophysical Research*, Vol. 109, C06025, doi:10.1029/2003JC002160, 2004.

Ruggiero, P., Kaminsky, G.M., Gelfenbaum, G., Voigt, B., 2005. Seasonal to interannual morphodynamics along a high-energy dissipative littoral cell, *Journal of Coastal Research*, 21 (3), 553–578.

Ruggiero, P., Kaminsky, G.M., Gelfenbaum, G., 2003a. Linking proxy-based and datum-based shorelines on a high-energy coastline: implications for shoreline change analyses, *Journal of Coastal Research*, SI 38, 57–82.

Ruggiero, P., Kaminsky, G.M., Komar, P.D., McDougal, W.G., 1997. Extreme waves and coastal erosion in the Pacific Northwest, *Proceedings of Waves '97*, 947–961.

Ruggiero, P., List, J.H., in press. Improving accuracy and statistical reliability of shoreline position and change estimates, *Journal of Coastal Research*.

Satake, K., Shimazaki, K., Tsuji, Y., Ueda, K., 1996. Time and size of a giant earthquake in Cascadia inferred from Japanese tsunami records of January 1700, *Nature*, 379, 246–249.

Schwab, W.C., Thieler, E.R., Allen, J.R., Foster, D.S., Swift, B.A., Denny, J.F., 2000. Influence of inner-continental shelf geologic framework on the evolution and behavior of the barrier-island system between Fire Island Inlet and Shinnecock Inlet, Long Island, New York, *Journal of Coastal Research*, 16, 408–422.

Sherwood, C.R., Gelfenbaum, G., Howd, P.A., Palmsten, M.L., 2001. Sediment transport on a high-energy ebb-tidal delta, *Proceedings of the 4th Conference on Coastal Dynamics*, 473–482.

Sherwood, C.R., Jay, D.A., Harvey, R.B., Hamilton, P., Simenstad, C.A., 1990. Historical Changes in the Columbia River Estuary, *Progress in Oceanography*, 25, 299–352.

Sherwood, C.R., Lacy, J.R., Voulgaris, G., 2006. Shear velocity estimates on the inner shelf off Grays Harbor, Washington, USA, *Continental Shelf Research*, 26, 1995–2018.

Short, A.D., 2003. Sediment transport around Australia – sources, mechanisms, rates, and barrier forms, *Proceedings of Coastal Sediments '03*, East Meets West Productions, CD-ROM, 11 pp.

Smith, D.G., Meyers, R.A., Jol, H.M., 1999. Sedimentology of an upper-mesotidal (3.7 m) Holocene barrier, Willapa Bay, SW Washington, U.S.A., *Journal of Sedimentary Research*, 69 (6), 1290–1296.

Smith, J.D., Hopkins, T.S., 1972. Sediment transport on the continental shelf off Washington and Oregon in light of recent current meter measurements, in: Swift, D.J.P., Duane, D.B., Pilkey, O.H. (Eds.), Shelf Sediment Transport: Processes and Patterns, Dowden, Hutchinson and Ross, Stroudsburg, 143–180.

Spahn, E.Y., Horner-Devine, A.R., Nash, J.D., Jay, D. A., Kilcher, L., in press. Particle re-suspension in the Columbia River plume near-field, *Journal of Geophysical Research*.

Sternberg, R.W., 1986. Transport and accumulation of river-derived sediment on the Washington continental shelf, USA, *Journal of the Geological Society*, London, 143, 945–956.

Sternberg, R.W., Creager, J.S., Johnson, J., Glassley, W., 1979. Stability of dredged material deposited seaward of the Columbia River mouth, in: Palmer, H.D., Gross, M.G. (Eds.), Ocean Dumping and Marine Pollution: Geological Aspects of Waste Disposal, Dowden, Hutchinson and Ross, Stroudsburg, pp. 17-49.

Sternberg, R.W., McManus, D.A., 1972. Implications of sediment dispersal from long-term bottom-current measurements on the continental shelf of Washington, in: Swift, D.J.P., Duane, D.B., Pilkey, O.H. (Eds.), Shelf Sediment Transport: Processes and Patterns, Dowden, Hutchinson and Ross, Stroudsburg, pp. 181–194.

Stive, M.J.F., Capobianco, M., Wang, Z.B., Ruol, P., Buijsman, M.C., 1998. Morphodynamics of a tidal lagoon and the adjacent coast, *Eighth International Biennial Conference on Physics of Estuaries and Coastal Seas*, Rotterdam, Balkema, 97–407.

Stive, M.J.F., de Vriend, H.J., 1995. Modelling shoreface profile evolution, *Marine Geology*, 126, 235–248.

Stive, M.J.F., Roelvink, D.J.A., de Vriend, H.J., 1991. Large-scale coastal evolution concept, *Proceedings of the 22nd International Conference on Coastal Engineering*, 1962–1974.

Styles, R., 2006. Application of a bottom boundary layer model in contrasting wave and current environments: Grays Harbor, Washington, *Journal of Waterway, Port, Coastal and Ocean Engineering*, 132 (5), 379–387.

Swift, D.J.P., 1976. Continental shelf sedimentation, in: Stanley, D.J., Swift, D.J.P. (Eds.), Marine Sediment Transport and Environmental Management, John Wiley and Sons, New York, pp. 311–350.

Swift, D.J.P., Thorne, J.A., 1991. Sedimentation on continental margins, I: a general model for shelf sedimentation, in: Swift, D.J.P., Oertel, G.F., Tillman, R.W., Thorne, J.A. (Eds.), Shelf Sand and Sandstone Bodies - Geometry, Facies and Sequence

Stratigraphy, Special Publication No. 14 of the International Association of Sedimentologists, Blackwell Scientific Publications, Oxford, pp. 3–31.

Terich, T., Levenseller, T., 1986. The Severe Erosion of Cape Shoalwater, Washington. *Journal of Coastal Research*, 2 (4), 465–477.

Thom, B.G., 1984. Transgressive and regressive stratigraphies of coastal sand barriers in eastern Australia, *Marine Geology*, 56, 137–158.

Tillotson, K.J., Komar, P.D., 1997. The wave climate of the Pacific Northwest (Oregon and Washington): a comparison of data sources, *Journal of Coastal Research*, 13, 440–452.

Twichell, D.C., Cross, V.A., 2001. Holocene evolution of the Southern Washington and Northern Oregon shelf and coast: Geologic discussion and GIS data release. *USGS Open-File Report OF 01-076*, 28 pp. (with CD).

Twichell, D.C., Cross, V.A., Peterson, C.D., this issue. Partitioning of sediment on the shelf offshore of the Columbia River littoral cell, *Marine Geology*.

U.S. Army Corps of Engineers, 1997. Long Term Maintenance of the South Jetty at Grays Harbor, Washington, U.S. Army Corps of Engineers Seattle District, Seattle, Washington, USA.

U.S. Army Corps of Engineers, 1999. Integrated Feasibility Report for Channel Improvements and Environmental Impact Statement, Columbia & Lower Willamette River Federal Navigation Channel, Portland District, Portland, Oregon, USA.

U.S. Army Corps of Engineers, 2009. MCR Dredged Material Disposal Site Annual Use Plan for 2009, U.S. Army Corps of Engineers, Portland District, and U.S. Environmental Protection Agency, Region 10.

Vanderburgh, S., Roberts, M.C., Peterson, C.D., Phipps, J.B., Herb, A., this issue. Transgressive and regressive deposits forming barriers and beachplains of the Columbia River littoral cell, USA, *Marine Geology*.

Venkatarathnam, K., McManus, D.A., 1973. Origin and distribution of sands and gravels on the northern continental shelf off Washington, *Journal of Sedimentary Petrology*, 43 (3), 799–811.

Walstra, D.-J., Ruggiero, P., Lesser, G., Gelfenbaum, G., 2005. Modeling nearshore morphological evolution at seasonal scale, *Proceedings of the 5th Conference on Coastal Dynamics*, CD-ROM, 13 pp.

Walter, S.R., Roy, E.H., Creager, J.S., Borgeld, J.C., 1979. An investigation to determine the bedload and suspended load transport over the outer tidal delta and monitor the sedimentary environment at Sites A, E, and D near the mouth of the Columbia River, U.S. Army Corps of Engineers, Portland District, Portland, Oregon.

Woxell, L.K., 1998. Prehistoric beach accretion rates and long-term response to sediment depletion in the Columbia River littoral system, USA, MS Thesis, Portland State University, Portland, Oregon, 206 pp.

Wright, L.D., Madsen, O.S., Chisholm, T.A., Xu, J.P., 1994. Inner continental shelf transport processes: the Middle Atlantic Bight, *Proceedings of Coastal Dynamics '94*, 867–878.

Wright, L.D., Short, A.D., 1983. Morphodynamics of beaches and surf zones in Australia, in: Komar, P.D. (Ed.), Handbook of Coastal Processes and Erosion, Boca Raton, Florida, CRC Press, pp. 35–64.

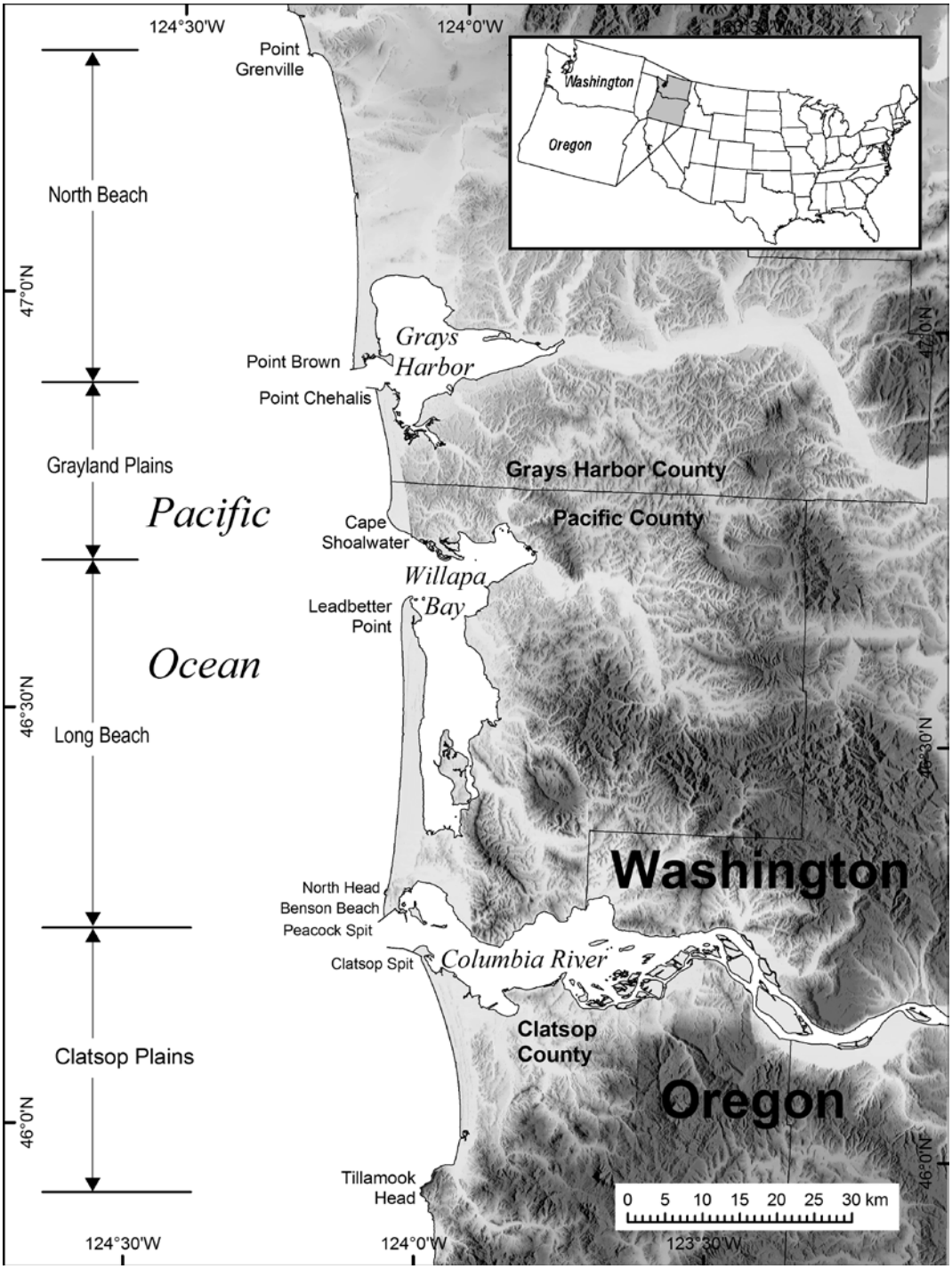

Figure 1. The Columbia River littoral cell spans 165 km along the U.S. Pacific Northwest coast of northwest Oregon and southwest Washington.

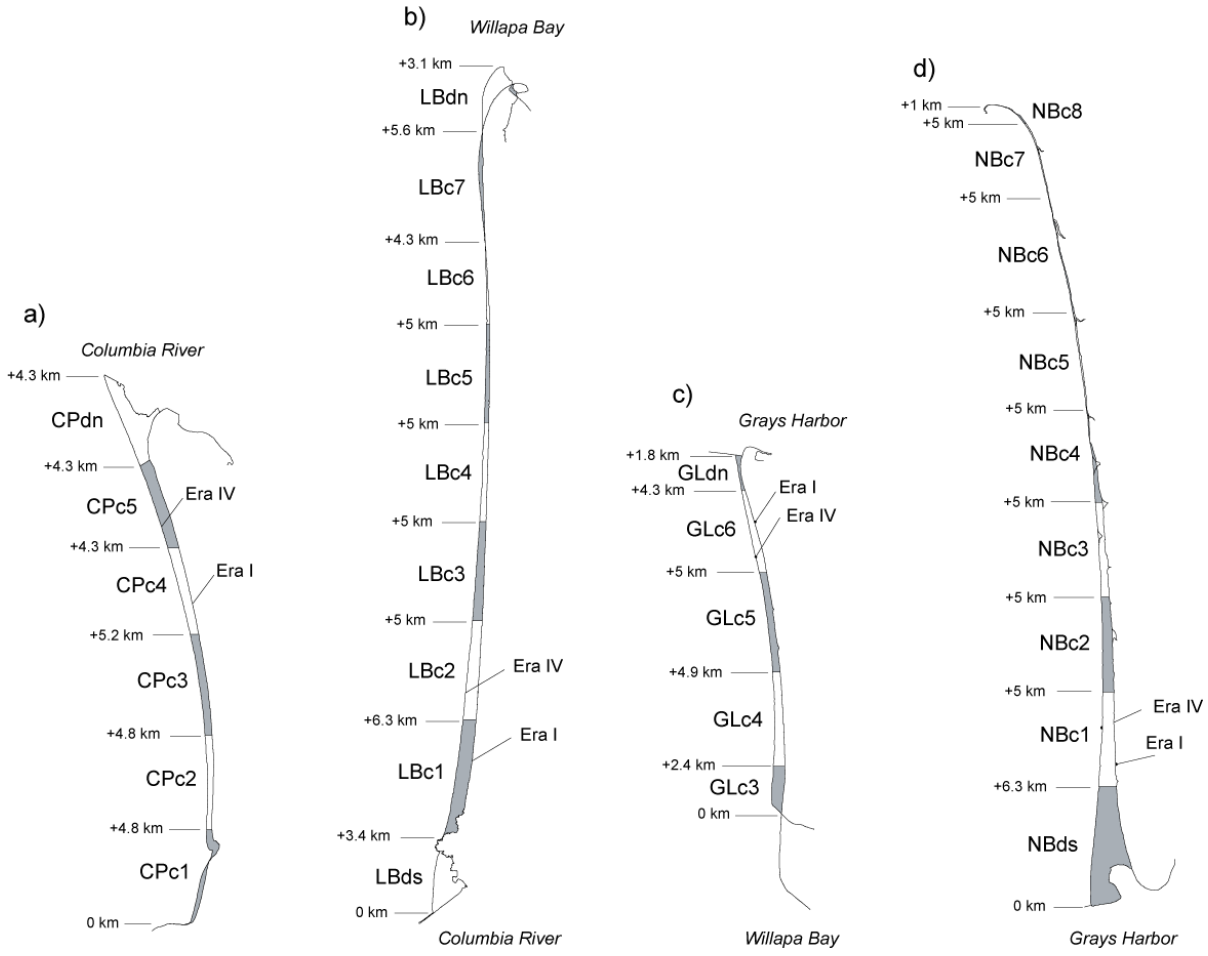

Figure 2. Plan view of a) Clatsop Plains (CP) , b) Long Beach (LB), c) Grayland Plains (GL) and d) North Beach (NB) showing the compartments, compartment names, and compartment lengths as a function of Northing; 'c' indicates coast, 'd' delta, 'n' north, and 's' south. The landward and seaward extent of the compartments is indicated by the Era I (1870s) and Era IV (1999) shorelines.

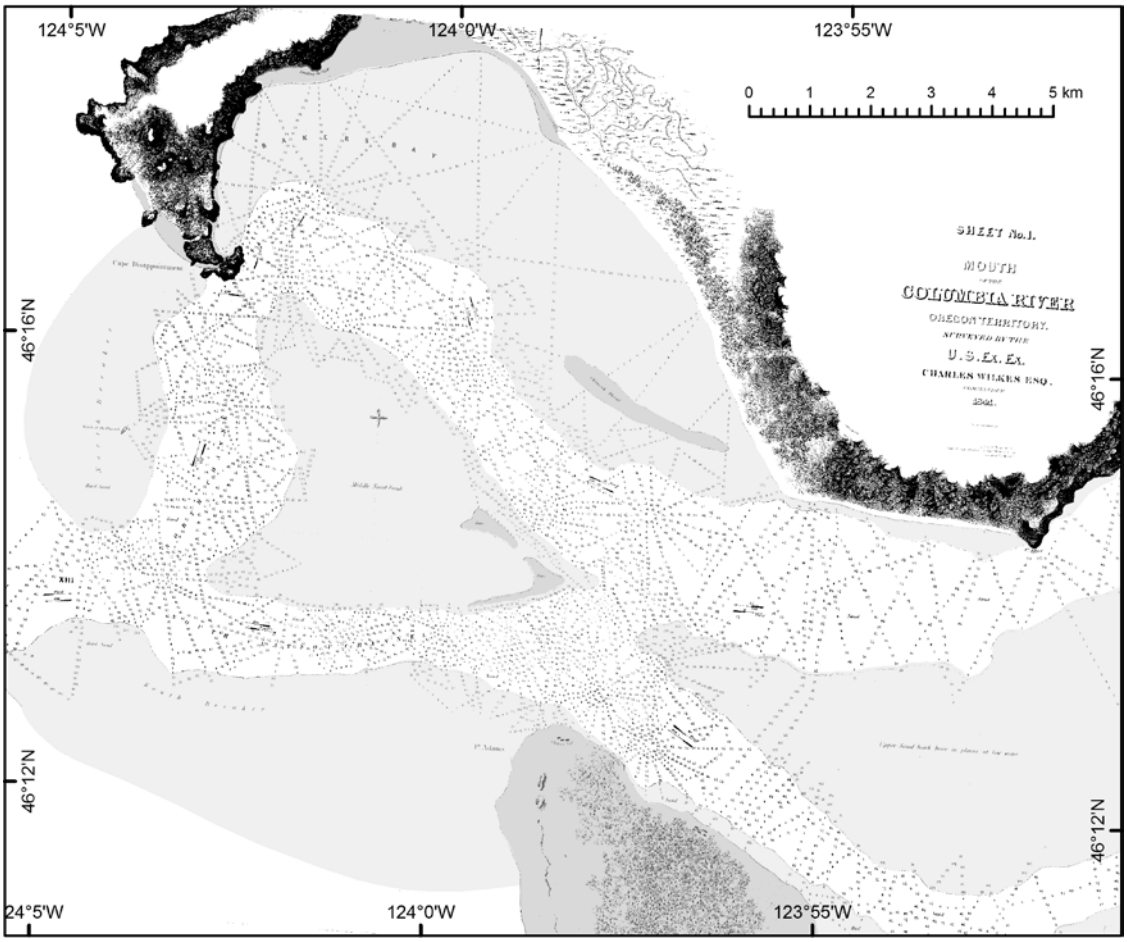

Figure 3. 1841 U.S. Exploring Expedition survey – Mouth of the Columbia River.

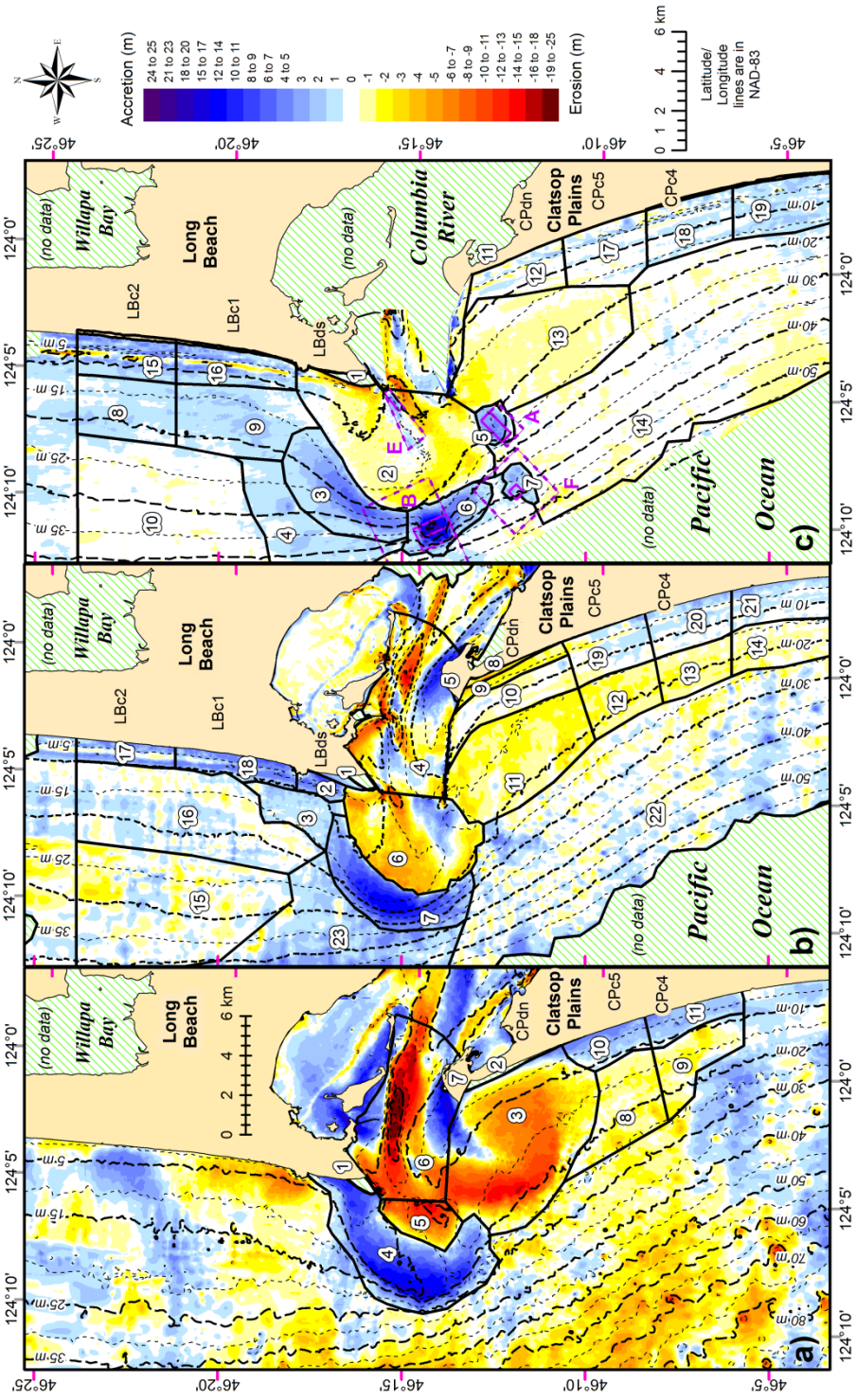

Figure 4. Mouth of the Columbia River and adjacent coast bathymetric change between: (a) 1868 and 1926; (b) 1926 and 1958; and (c) 1958 and 1999.

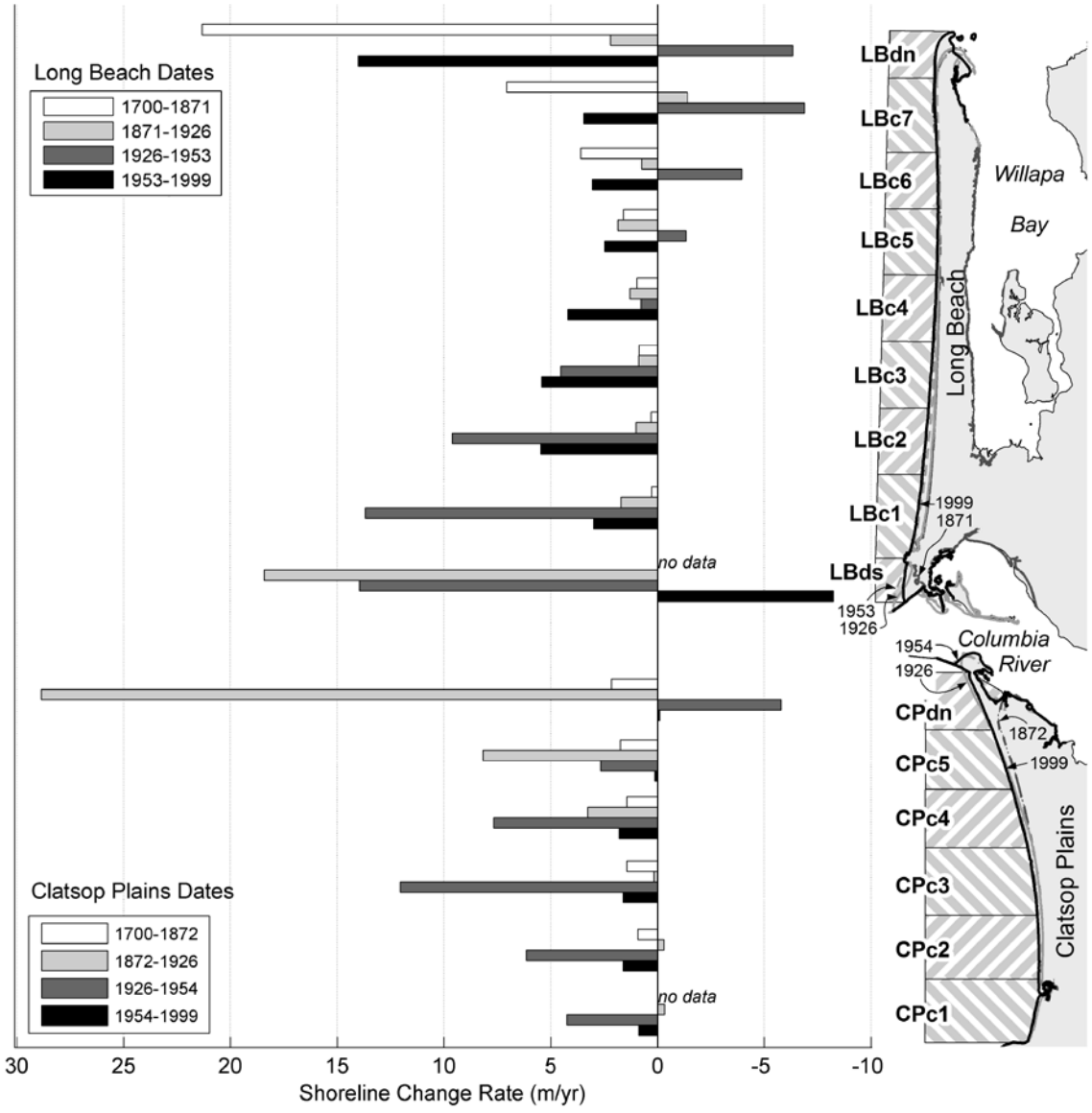

Figure 5. Compartment-averaged shoreline-change rates at Clatsop Plains and Long Beach.

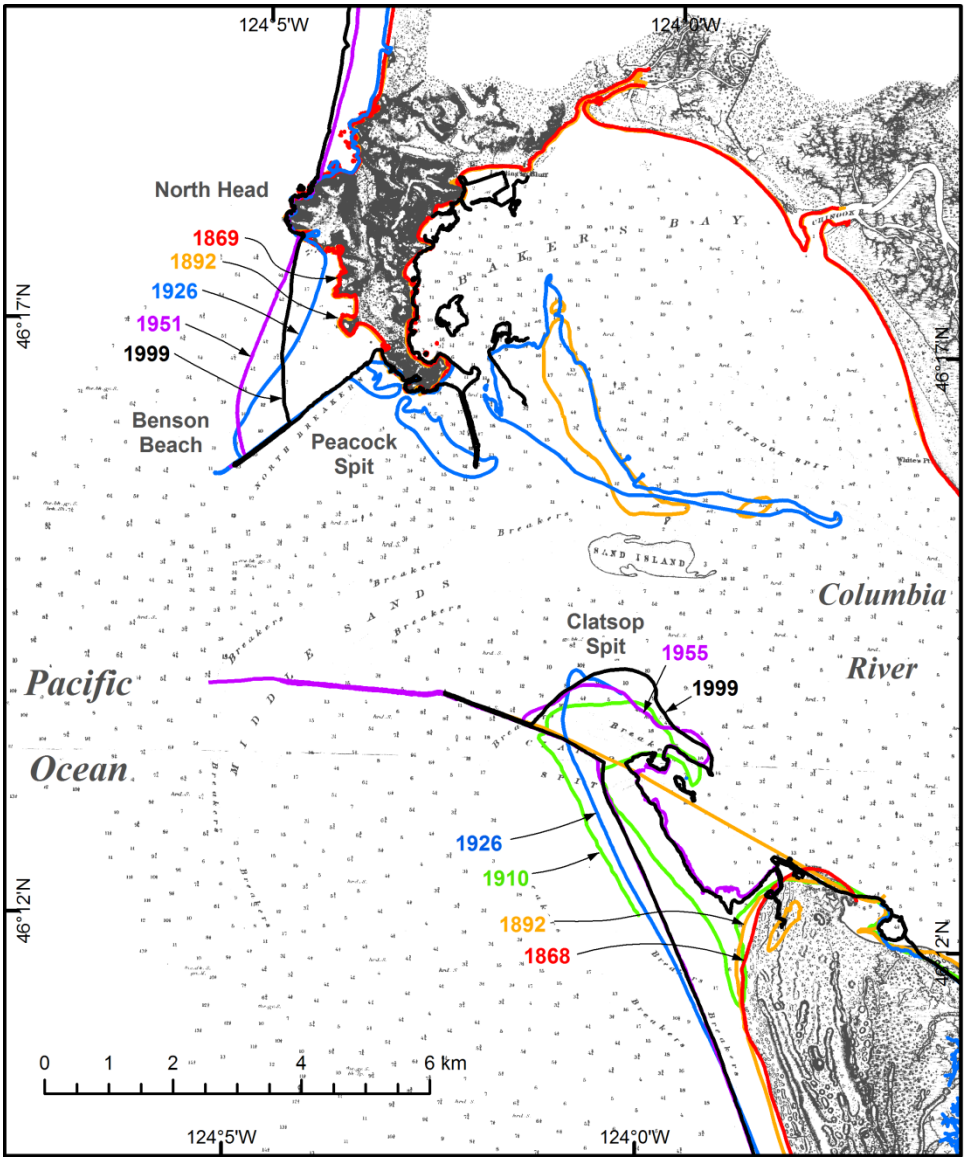

Figure 6. 1870 U.S. Coast and Geodetic Survey – Mouth of the Columbia River, with historical shorelines.

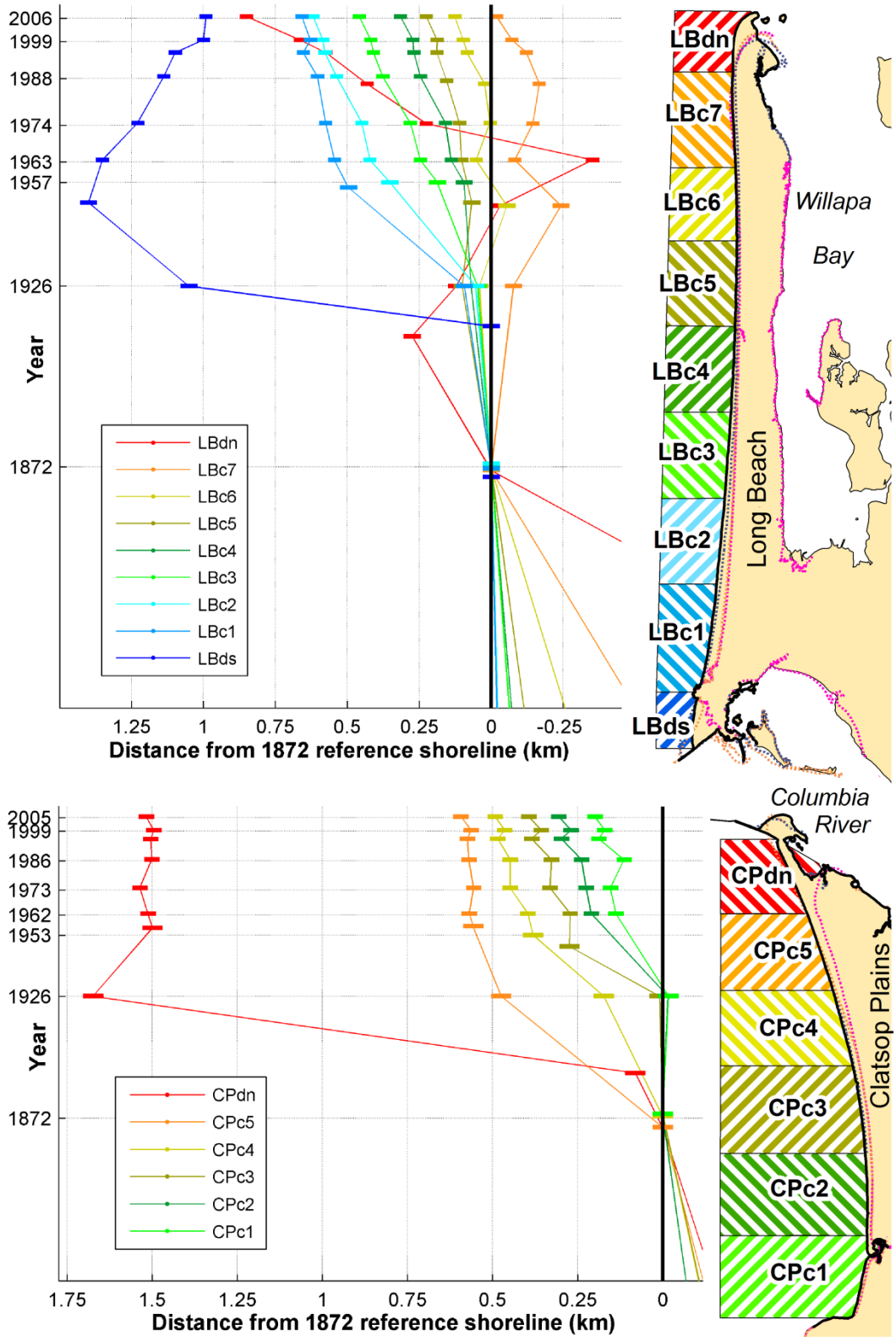

Figure 7. Compartment-averaged historical shoreline positions at Clatsop Plains and Long Beach relative to the 1870s shoreline position. Horizontal bars indicate shoreline position uncertainty described in the text.

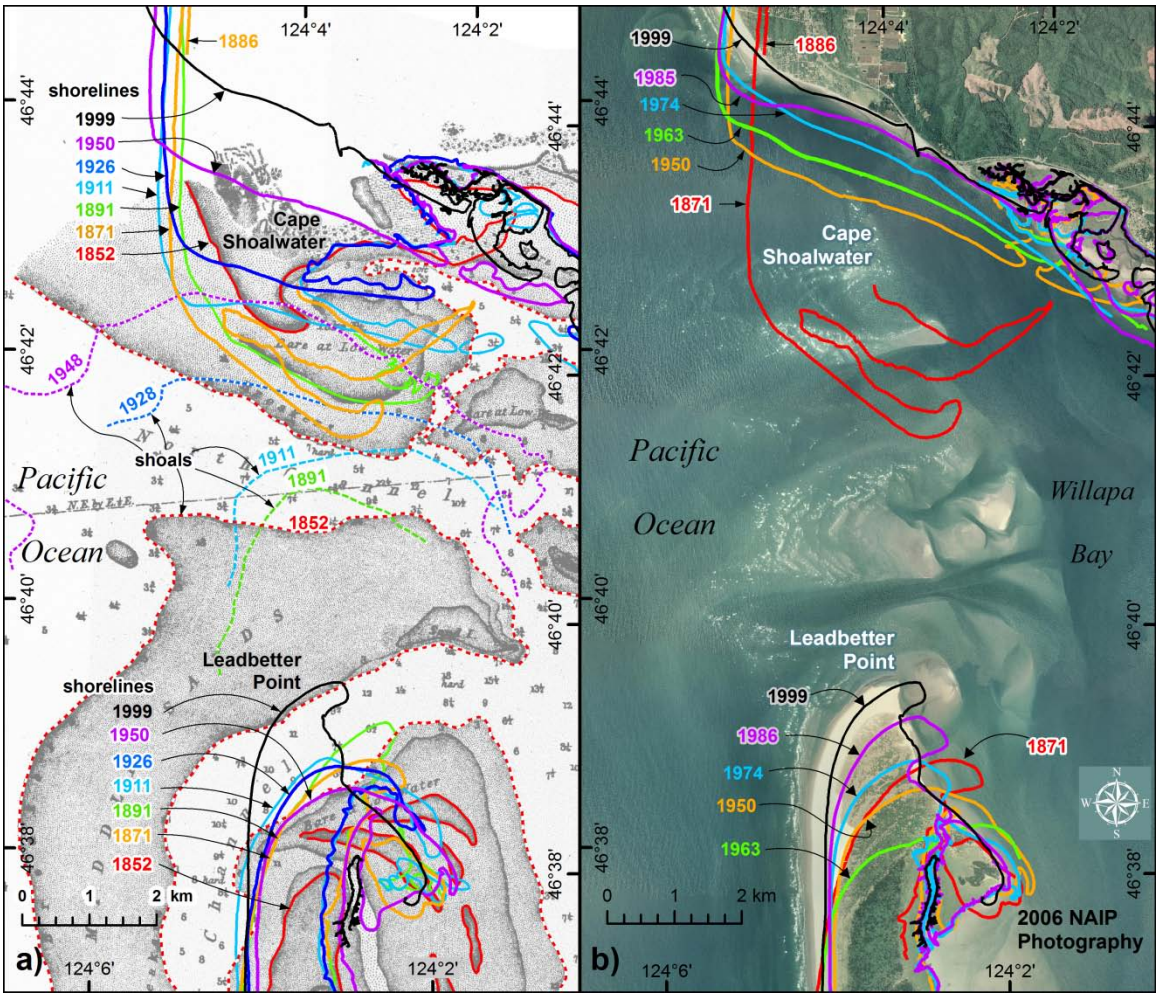

Figure 8. Mouth of Willapa Bay a) historical shoreline change and shoal migration on the 1852 U.S. Coast Survey chart, and b) historical shoreline change on a 2006 aerial photomosaic. Shoal position is delineated by the 5.5-m depth contour.

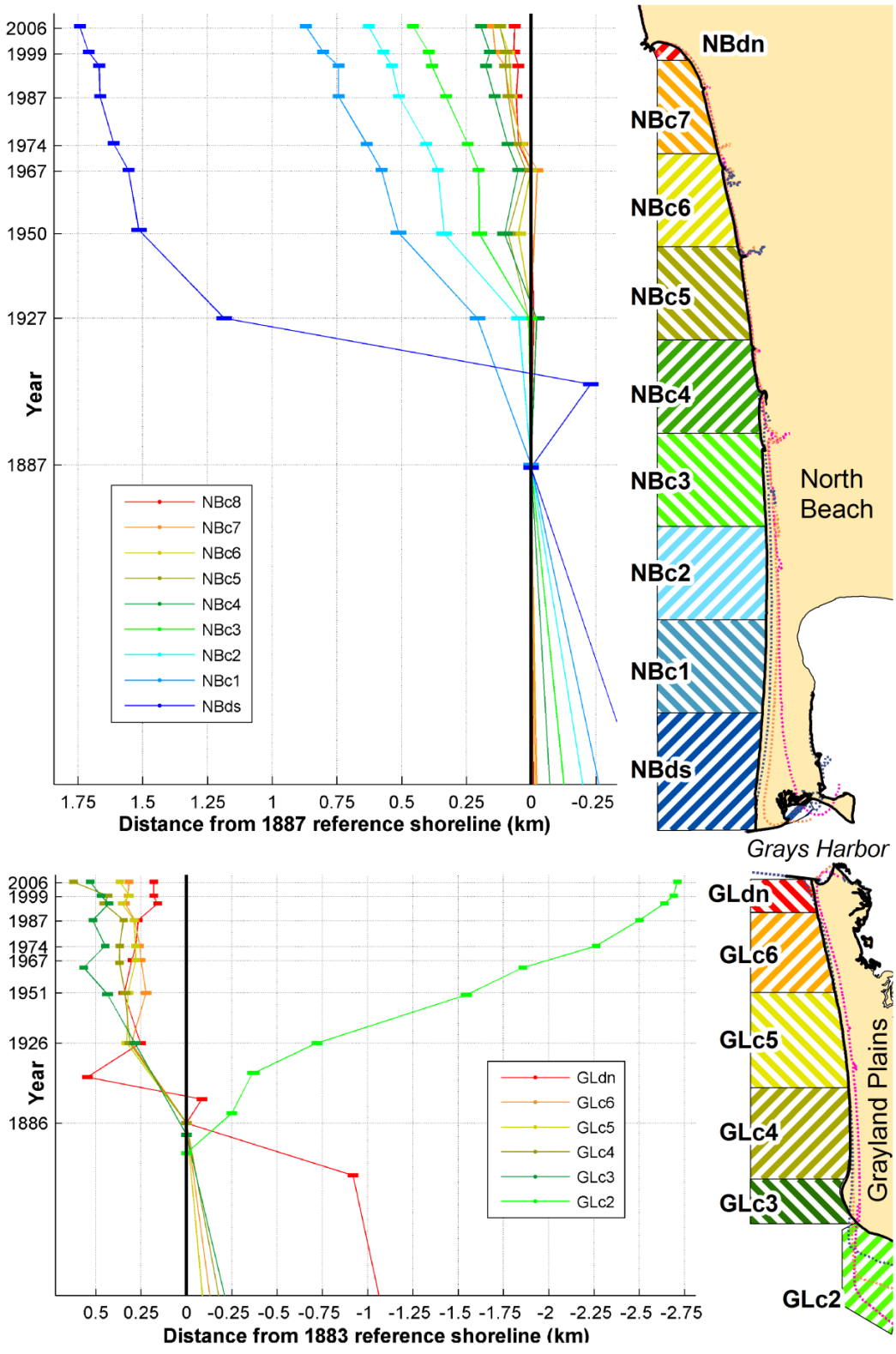

Figure 9. Compartment-averaged historical shoreline positions at Grayland Plains and North Beach. Horizontal bars indicate shoreline position uncertainty described in the text.

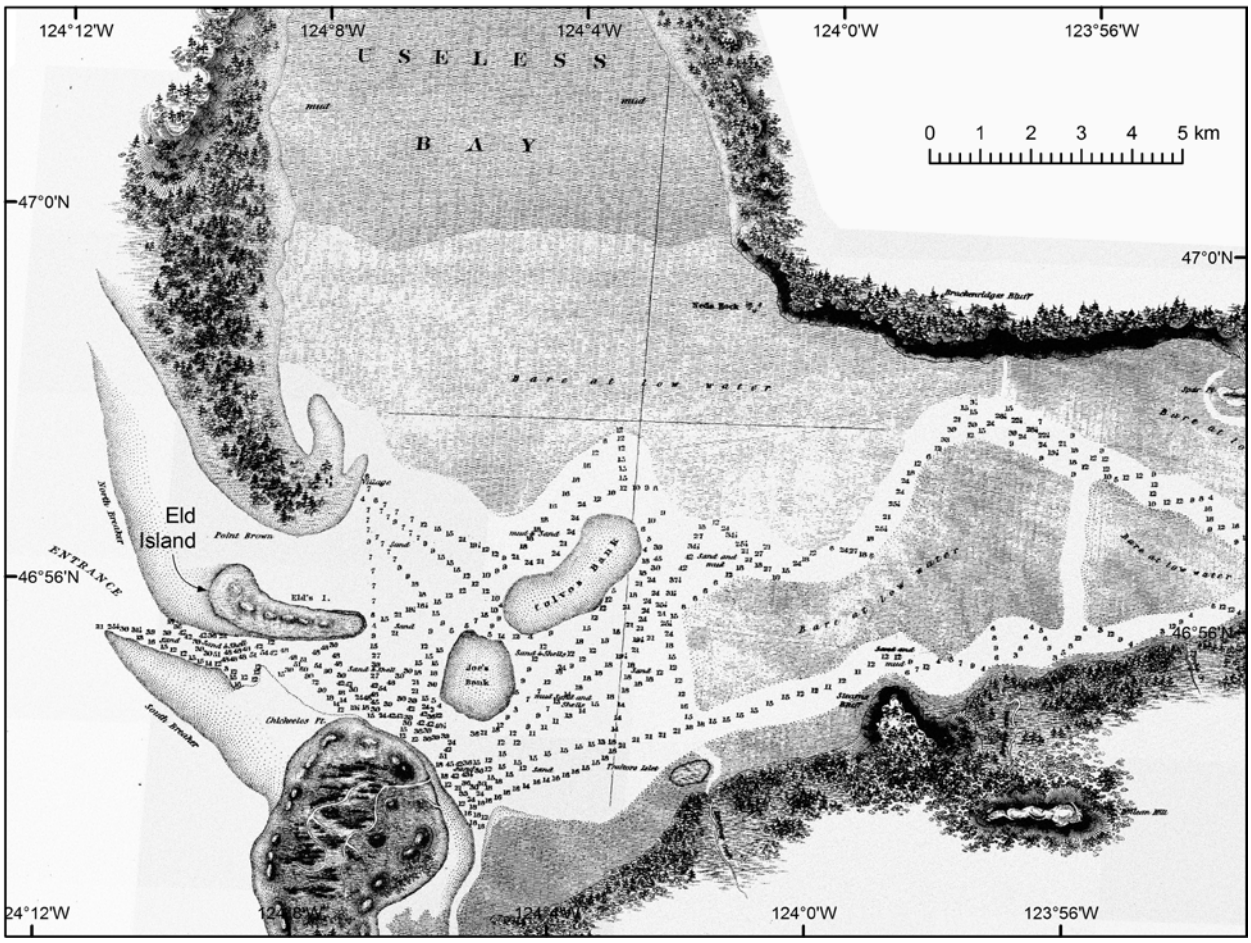

Figure 10. 1841 U.S. Coast Survey – Mouth of Grays Harbor.

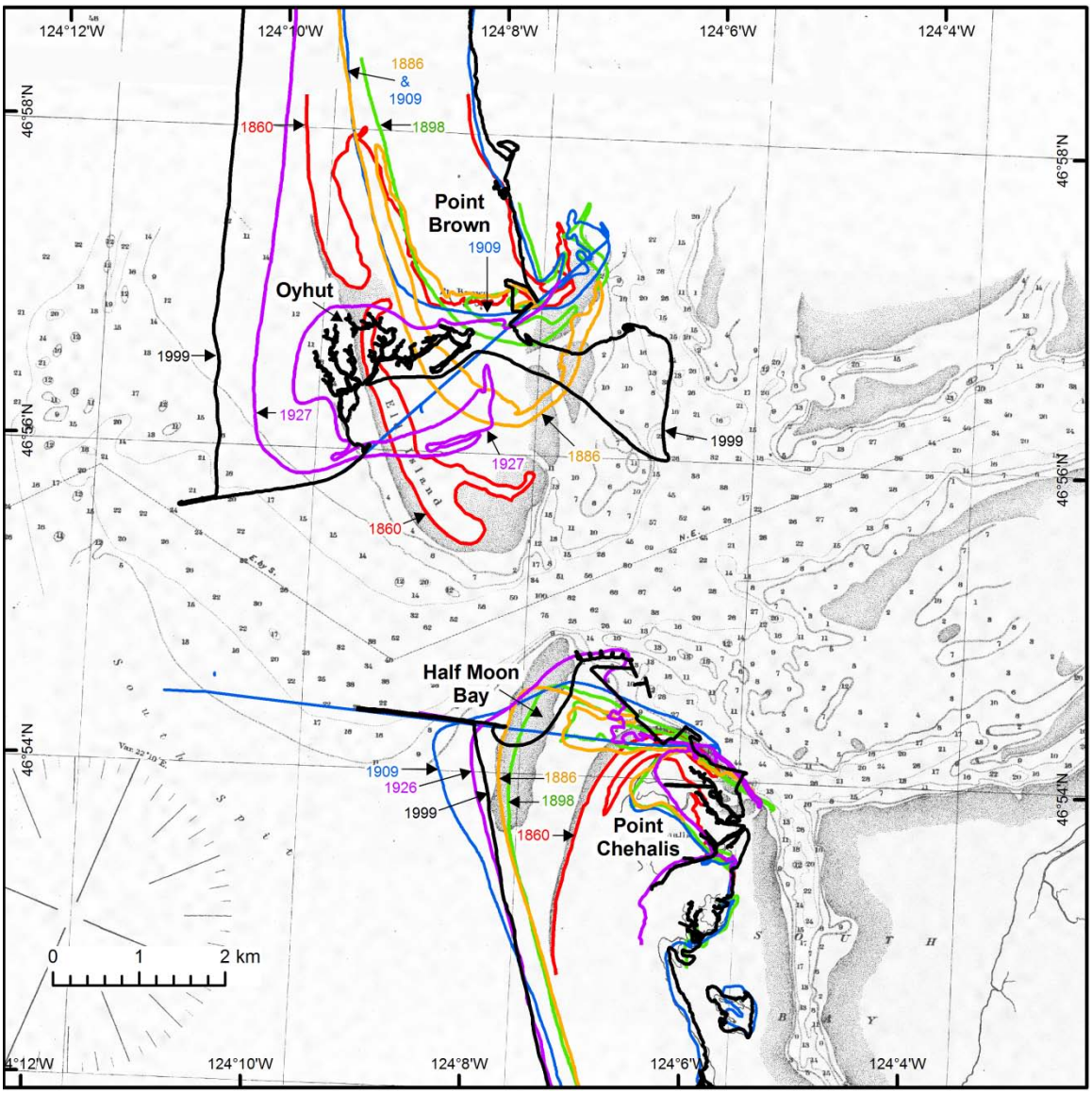

Figure 11. 1860 U.S. Coast Survey – Mouth of Grays Harbor, with historical shorelines.

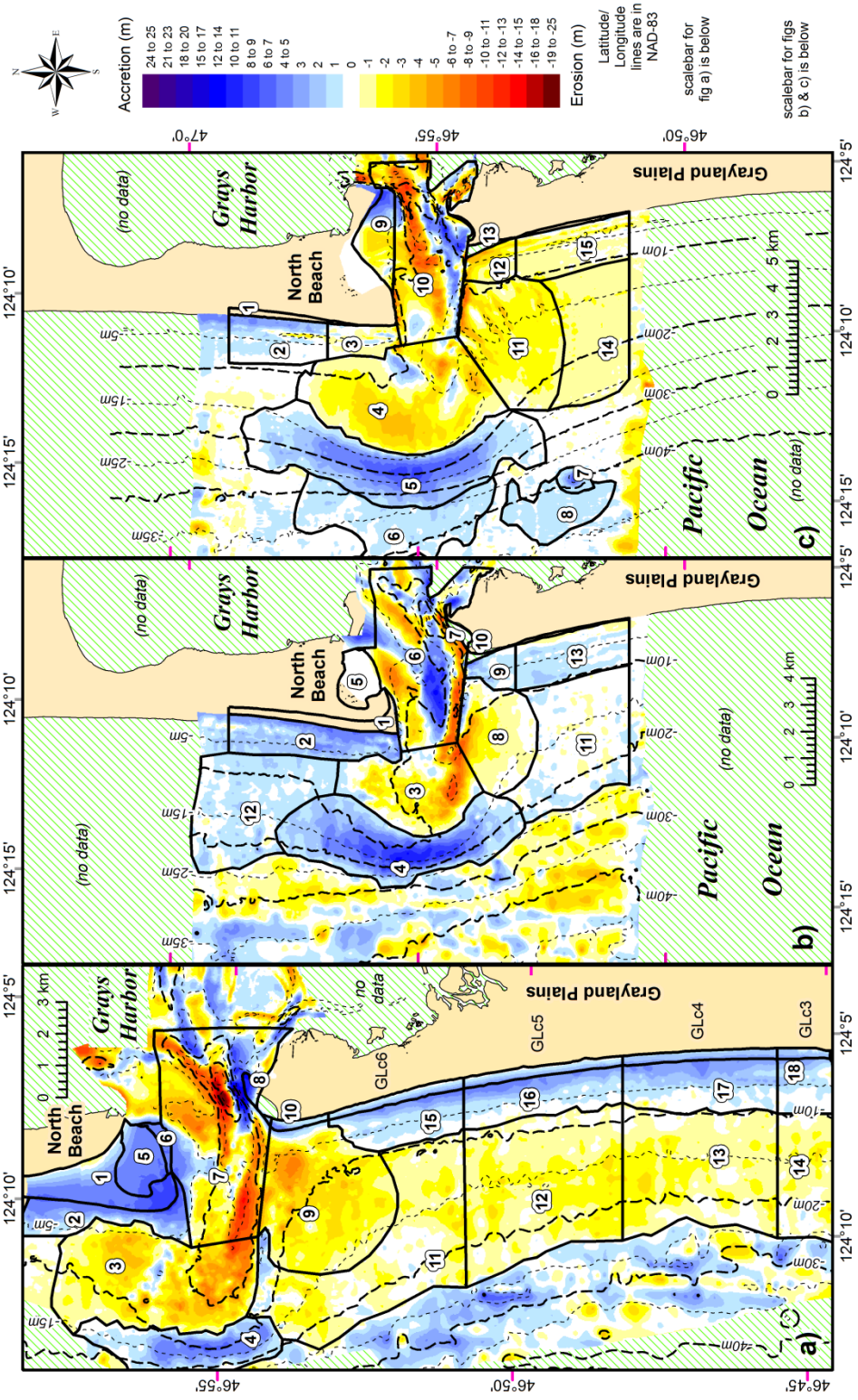

Figure 12. Mouth of Grays Harbor and adjacent coast bathymetric change between a) 1893 and 1926, b) 1926 and 1954, and c) 1954 and 1999. Circled numbers refer to compartments described in the text.

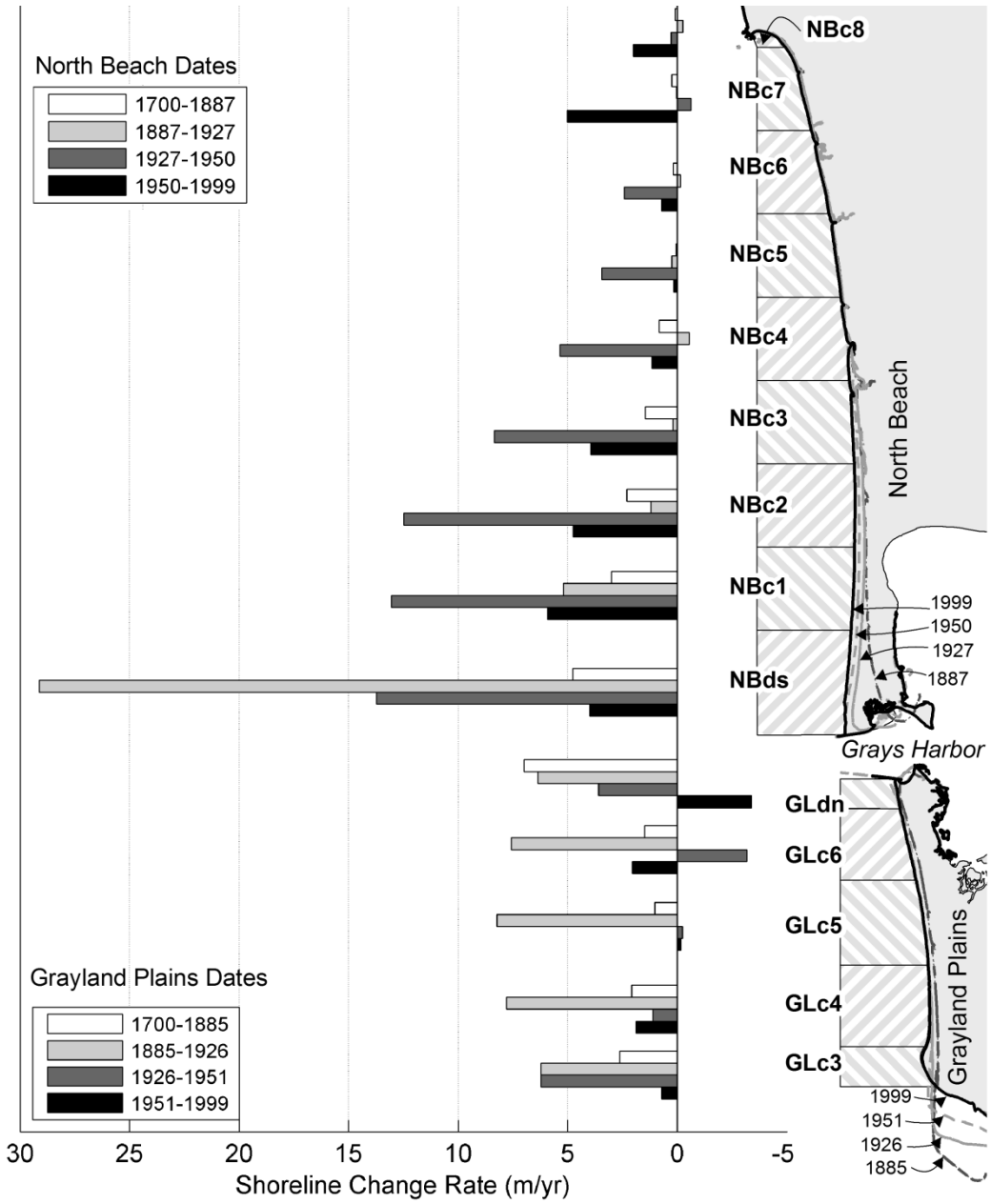

Figure 13. Compartment-averaged shoreline-change rates at Grayland Plains and North Beach.

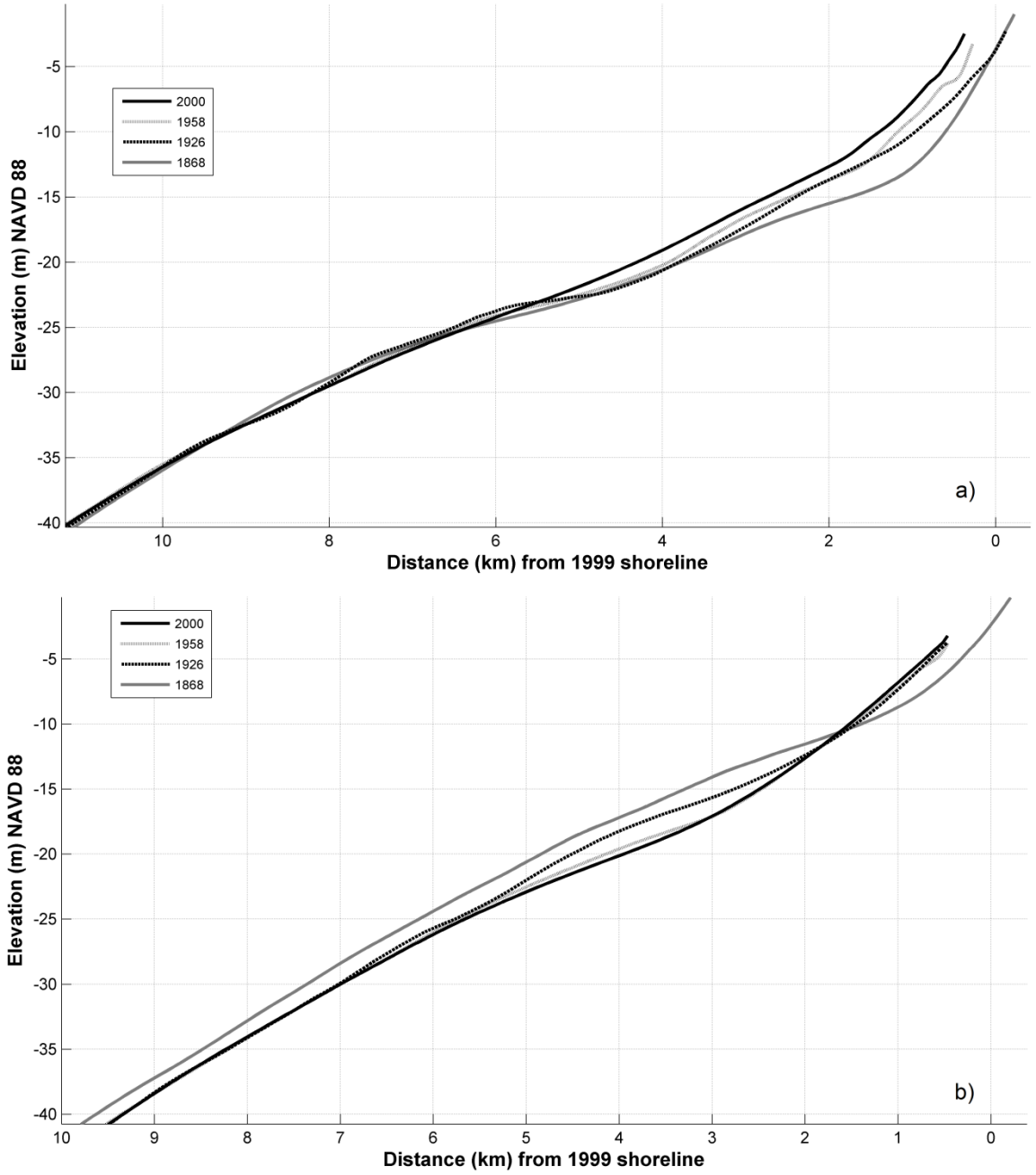

Figure 14. Historical shoreface profile change at a) southern Long Beach (LBc2), and b) northern Clatsop Plains (CPc5). Profiles are alongshore-averaged and cross-shore smoothed.

Table 1. Shoreline and bathymetry dates. Shoreline dates are compartment-averaged and bathymetry dates are representative of merged survey data.

		Shoreline Dates											Bathymetry Dates			
		Supple-mental	Era I	*Supplemental*		Era II	Era III	*Supplemental*				Era IV	Era I	Era II	Era III	Era IV
North Beach	NBc8		1887			1927	*no data*	1967	1974	1987	1995	1999				
	NBc7		1887			1927	*no data*	1967	1974	1987	1995	1999				
	NBc6		1887			1927	1950	1967	1974	1987	1995	1999				
	NBc5		1887			1927	1950	1967	1974	1987	1995	1999				
	NBc4		1887			1927	1950	1967	1974	1987	1995	1999				
	NBc3		1887			1927	1950	1967	1974	1987	1995	1999				
	NBc2		1887			1927	1950	1967	1974	1987	1995	1999	*The dates listed below apply to the whole estuary & sub-cell complex*			
	NBc1		1887			1927	1950	1967	1974	1987	1995	1999				
	NBds	1860	1886	1898	1909	1927	1951	1967	1974	1987	1995	1999	1887	1926	1954	1999
	Average		1887			1927	1950					1999	1900	1927		
Grayland Plains	GLdn	1860	1886	1898	1909	1926	1951	1967	1974	1987	1995	1999				
	GLc6	1860	1886	1898	1909	1926	1951	1967	1974	1987	1995	1999				
	GLc5		1886			1926	1951	1967	1974	1987	1995	1999				
	GLc4		1886			1926	1951	1966	1974	1987	1995	1999				
	GLc3		1880	1891	1911	1926	1950	1963	1974	1987	1995	1999	simplified dates used:			
	Average		1885			1926	1951					1999	1893	1926	1954	1999
Long Beach	LBdn		1871	1891	1911	1926	1950	1963	1974	1986	1995	1999				
	LBc7		1871			1926	1950	1963	1974	1986	1995	1999				
	LBc6		1871			1926	1950	1963	1974	1986	1995	1999				
	LBc5		1872			1926	1951	1963	1974	1987	1995	1999				
	LBc4		1872			1926	1957	1963	1974	1988	1995	1999	*The dates listed below apply to the whole estuary & sub-cell complex*			
	LBc3		1873			1926	1957	1963	1974	1988	1995	1999				
	LBc2		1873			1926	1957	1963	1974	1988	1995	1999	1868	1926	1958	1998
	LBc1		1871			1926	1955	1963	1974	1988	1995	1999	1877			2000
	LBds		1869		1914	1926	1951	1963	1974	1988	1995	1999	1887			
	Average		1871			1926	1953					1999				
Clatsop Plains	CPdn		1868	1892		1926	1956	1962	1973	1986	1995	1999				
	CPc5		1868	1892		1926	1957	1962	1973	1986	1995	1999				
	CPc4		1872	1892		1926	1953	1962	1973	1986	1995	1999				
	CPc3		1874			1926	1948	1962	1973	1986	1995	1999				
	CPc2		1874			1926	*no data*	1962	1973	1986	1995	1999				
	CPc1		1874			1926	*no data*	1962	1973	1986	1995	1999	simplified dates used:			
	Average		1872			1926	1954					1999	1868	1926	1958	1999

Table 2. History of Jetty Construction at the MCR and the MGH.

Columbia River Jetty Construction (Hickson and Rodolf, 1950)		
1885 – 1895	South Jetty construction	Length 7200 m; height +3.7 m MLLW at shore to +1.2 m MLLW at outer end
1903 – 1913	South Jetty extension	Extension 3400 m; +3 m to +7.3 m MLLW
1913 – 1917	North Jetty construction	Length 3781 m; height from +8.5 m to 9.6 m MLLW
Grays Harbor Jetty Construction (USACE, 1997)		
1898 – 1902	South Jetty construction	Length 4186 m; height +2.4 m MLLW;
1907 – 1916	North Jetty construction	Length 5244 m; height +2.4 m MLLW

Table 3. Upper shoreface and barrier volume-change rates. Triangles indicate volume-change rate for above MHW only.

	Volume Change Rates ($m^3/yr\ m^{-1}$)					
Compartment	**Interval 1**		**Interval 2**		**Interval 3**	
Grenville (NBc8)	1893 → 1926	***	1926 → 1954	***	1954 1999	-13.2
Copalis NWR (NBc7)	1893 → 1926	-0.2	1926 → 1954	***	1954 → 1999	0.0
Moclips (NBc6)	1893 → 1926	-6.6	1926 → 1954	24.2	1954 → 1999	-0.7
Roosevelt Beach (NBc5)	1893 → 1926	5.5	1926 → 1954	39.0	1954 → 1999	-6.7
Copalis River mouth (NBc4)	1893 → 1926	-7.0	1926 → 1954	55.1	1954 → 1999	11.8
Connor Creek mouth (NBc3)	1893 → 1926	3.9	1926 → 1954	96.5	1954 → 1999	47.5
Ocean City (NBc2)	1893 → 1926	23.9	1926 → 1954	151.4	1954 → 1999	58.1
City of Ocean Shores (NBc1)	1893 → 1926	87.2	1926 → 1954	159.7	1954 → 1999	66.6
Ocean Shores Jetty (NBds)	1893 → 1926	38.5▲	1926 → 1954	33.2▲	1954 → 1999	7.5▲
Westport Jetty (GLdn)	1893 → 1926	26.4	1926 → 1954	7.8▲	1954 → 1999	-7.9▲
Twin Harbors SP (GLc6)	1893 → 1926	88.2	1926 → 1954	23.5	1954 → 1999	-22.1
Grayland (GLc5)	1893 → 1926	100.0	1926 → 1954	-2.3	1954 → 1999	7.0
Grayland Beach SP (GLc4)	1893 → 1926	105.2	1926 → 1954	11.2	1954 → 1999	29.3
Cape Shoalwater (GLc3)	1893 → 1926	58.6	1926 → 1954	48.6	1954 → 1999	36.6
North Cove (GLc2)	1893 → 1926	***	1926 → 1954	***	1954 → 1999	***
West side Willapa NWR (LBdn)	1868 → 1926	6.6	1926 → 1958	-41.8	1958 → 1999	83.3
North end Leadbetter SP (LBc7)	1868 → 1926	-17.7	1926 → 1958	-65.4	1958 → 1999	55.0
Oysterville (LBc6)	1868 → 1926	9.6	1926 → 1958	-40.3	1958 → 1999	60.1
Ocean Park & Airstrip (LBc5)	1868 → 1926	28.0	1926 → 1958	-16.8	1958 → 1999	60.8
Klipsan Beach (LBc4)	1868 → 1926	19.5	1926 → 1958	12.4	1958 → 1999	84.9
Loomis Lake SP (LBc3)	1868 → 1926	13.3	1926 → 1958	72.3	1958 → 1999	110.5
Breakers Lake (LBc2)	1868 → 1926	14.7	1926 → 1958	145.9	1958 → 1999	110.7
Long Beach & Seaview (LBc1)	1868 → 1926	18.6	1926 → 1958	193.9	1958 → 1999	67.3
Cape Disappointment (LBds)	1868 → 1926	39.3▲	1926 → 1958	32.4▲	1958 → 1999	-22.8▲
Clatsop Spit-south of Jetty (CPdn)	1868 → 1926	37.7▲	1926 → 1958	-17.5▲	1958 → 1999	0.2▲
Warrenton (CPc5)	1868 → 1926	121.0	1926 → 1958	26.5	1958 → 1999	16.4
Camp Rilea (CPc4)	1868 → 1926	79.7	1926 → 1958	102.1	1958 → 1999	47.0
Surf Pines (CPc3)	1868 → 1926	2.6	1926 → 1958	121.6	1958 → 1999	86.0
Delray (CPc2)	1868 → 1926	-4.4	1926 → 1958	107.4	1958 → 1999	76.0
Seaside (CPc1)	1868 → 1926	-7.6	1926 → 1958	43.7	1958 → 1999	30.9

▲ = above Mean High Water only

Table 4. Comparison of late prehistoric and historical shoreline change rates.

Compartment	Late Prehistoric (1700–1870s) Change Rate (m/yr)			Historical (1870s–1999) Change Rate (m/yr)		
Grenville (NBc8)	0.1			0.6		
Copalis NWR (NBc7)	0.2	average		1.2	average	
Moclips (NBc6)	0.2		0.1	0.8		0.9
Roosevelt Beach (NBc5)	0.1			0.9		
Copalis River mouth (NBc4)	0.8			1.4		
Connor Creek mouth (NBc3)	1.5			3.5		
Ocean City (NBc2)	2.3	average	2.7	5.1	average	6.1
City of Ocean Shores (NBc1)	3.0			7.1		
Ocean Shores Jetty (NBds)	4.8			15.1		
Half Moon Bay	10.1			0.5		
Westport Jetty (GLdn)	7.0			1.6		
Twin Harbors SP (GLc6)	1.5	average		2.8	average	
Grayland (GLc5)	1.0		1.5	2.8		3.1
Grayland Beach SP (GLc4)	2.1			3.8		
Cape Shoalwater (GLc3)	2.6			4.0		
North Cove (GLc2)				-20.9		
Grassy Island (Leadbetter Point)	25.8			7.0		
West side Willapa NWR (LBdn)	21.3			5.2		
North end of Leadbetter SP (LBc7)	7.1			-0.6		
Oysterville (LBc6)	3.6			0.8		
Ocean Park & Airstrip (LBc5)	1.6			1.5		
Klipsan Beach (LBc4)	1.0	average	1.3	2.1	average	2.9
Loomis Lake State Park (LBc3)	0.9			3.3		
Breakers Lake (LBc2)	0.3			4.6		
Long Beach & Seaview (LBc1)	0.3			4.9		
Cape Disappointment (LBds)				7.7		
Fort Stevens State Park				34.7		
Clatsop Spit-south of Jetty (CPdn)	2.2			11.4		
Warrenton (CPc5)	1.7			4.3		
Camp Rilea (CPc4)	1.4	average	1.4	3.7	average	3.2
Surf Pines (CPc3)	1.4			2.8		
Delray (CPc2)	0.9			2.1		
Seaside (CPc1)				1.4		

Table 5. Comparison of strand plain accumulation and shoreface erosion at Grayland Plains and Clatsop Plains.

Grayland Plains			
	1893 – 1926	*1926 – 1954*	*1954 – 1999*
upper shoreface and strand plain	56.7 Mm^3 1.7 Mm^3/yr	11.8 Mm^3 0.4 Mm^3/yr	7.3 Mm^3 0.2 Mm^3/yr
mid- to lower shoreface	-71.9 Mm^3 -2.2 Mm^3/yr	-10.0 Mm^3 -0.4 Mm^3/yr	-53.9 Mm^3 -1.2 Mm^3/yr
Clatsop Plains			
	1868 – 1926	*1926 – 1958*	*1958 – 1999*
upper shoreface and strand plain	74.0 Mm^3 1.3 Mm^3/yr	47.2 Mm^3 1.5 Mm^3/yr	50.9 Mm^3 1.2 Mm^3/yr
mid- to lower shoreface	-247.2 Mm^3 -4.3 Mm^3/yr	-72.3 Mm^3 -2.3 Mm^3/yr	-59.8 Mm^3 -1.5 Mm^3/yr